DMD Fast Forward. Published on December 29, 2010 as doi:10.1124/dmd.110.037044

DMD # 037044

Metabolism of Gambogic Acid in Rats: a Rare Intestinal Metabolic Pathway Responsible for its Final Disposition

Jing Yang, Li Ding, Linlin Hu, Wenjuan Qian, Shaohong Jin, Xiaoping Sun, Zhenzhong Wang, and Wei Xiao

Department of Pharmaceutical Analysis, Key Laboratory of Drug Quality Control and Pharmacovigilance, China Pharmaceutical University, Nanjing, China (*J.Y., L.D, L.H, W.Q.*), National Institution for the Control of Pharmaceutical and Biological Products, China (*S.J.*), and Kanion Pharmaceutical Co., Ltd, Lianyungang, China (*X.S, Z.W, W.X.*)

DMD # 037044

Running title: Metabolism of gambogic acid in rats

Correspondence To:

Prof. Li Ding, Department of Pharmaceutical Analysis, China Pharmaceutical University, 24 Tongjiaxiang, Nanjing 210009, China.

E-mail: dinglidl@hotmail.com Tel: +86 025 83271289 Fax: +86 025 83271289

Prof. Shaohong Jin, National Institution for the Control of Pharmaceutical and Biological Products, Beijing 100050, China

E-mail: shaohongjin@gmail.com Tel: +86 010 67095258 Fax: +86 010 67095258

Number of text pages: 33

Number of Tables: 3

Number of Figures: 19 (including 9 supplemental figures)

Number of references: 41

Words in the abstract: 243

Words in the introduction (including references): 544

Words in the discussion (including references): 1413

Abbreviations: 10-α SGA, 10-α sulfonic acid GA, 10-β SGA, 10-β sulfonic acid GA; 10-GGA, 10-glutathionyl GA; GSH, glutathione; DAD, diode array detector; LC-MS/MS, Liquid Chromatography Tandem Mass Spectrometry; CID, collision-induced dissociation; NAC, N-acetylcysteine.

Abstract: Gambogic acid (GA) is a promising natural anticancer candidate. Although the anticancer activity of GA has been well demonstrated, information regarding the metabolic fate of GA is limited. Previous studies suggest that GA is mainly excreted into intestinal tract in rats through bile after i.v. administration, whereas only traces appeared in the feces, suggesting that GA is metabolized abundantly in the intestine. However, there is no report about the intestinal metabolism of GA either in animals or humans. In this study, two sulfonic acid metabolites of GA were found abundantly in the fecal samples of rats after i.v. administration and their structures were identified as 10-α sulfonic acid GA and 10-β sulfonic acid GA by comparison of the retention time and spectral data with those of synthesized reference substances using LC-DAD-MS/MS. This rare intestinal metabolic pathway mainly involves Michael addition of sulfite ion to the 9, 10 carbon-carbon double bond of α, β-unsaturated ketone. Additionally, a more detailed metabolic profile in rats is proposed according to the results of *in vitro* and *in vivo* studies. It is found that GA can be metabolized by a variety of routes, including mono-oxidation, hydration, glutathionylation, glucuronidation, glucosidation in the liver of rats. These findings provide information on the major metabolic soft spot of GA in the intestine and liver of rats, which is not only useful in the future human metabolic study of this compound, but also of value in the metabolic studies of GA analogues.

DMD Fast Forward. Published on December 29, 2010 as DOI: 10.1124/dmd.110.037044
This article has not been copyedited and formatted. The final version may differ from this version.

Introduction

During the past decades, inspired by the unusual caged skeleton and remarkable bioactivity of caged xanthones mainly derived from the Garcinia genus, scientists from various fields have shown increasing interest on these promising natural products, with gambogic acid (GA, Fig. 1) being the best representative (Han and Xu, 2009). GA is abundant in the resin of *Garcinia morella* and *Garcinia hanburyi* with a long history of use as a complementary and alternative medicine. The anti-tumor activity of GA has been well demonstrated, and recent work revealed that GA not only displayed potent anticancer effects against a wide range of human cancers, but also exhibited dramatic anti-multidrug resistance activity *in vitro* (Qin et al., 2007). All of these efforts favor GA as a promising anticancer candidate, and it is now under a phase II clinical trial in China.

It is well recognized that studies of drug metabolism have a vital role in the pharmaceutical industry and the identification of *in vitro* and *in vivo* drug metabolites is part of the discovery and development programs of pharmaceutical industry (Castro-Perez, 2007). Increasing demands on the discovery and development of this promising natural product for clinical therapy have challenged scientists to expedite the metabolic study of GA, and whereby provide information on the metabolic soft spots of this molecule which can be used in further medicinal chemistry efforts to optimize GA analogues. Although the pharmacokinetics of GA in rats (Hao et al., 2007a), dogs (Hao et al., 2007b; Yang et al., 2010a) and humans (Ding et al., 2007; Yang et al., 2010b) have been reported, the ultimatum fate of this natural product in all of these species was unclear. Only a few of incomplete metabolic studies of GA have been reported and no reports about the metabolism of other caged xanthones have appeared so far. *In vitro* and *in vivo* studies (Liu et al., 2006; Hao et al., 2007a)

indicate that GA can be metabolized to two phase I metabolites in rat liver and their structures are further elucidated as 10-hydroxygambogic acid and 9,10-epoxygambogic acid (Feng et al., 2007); (Zhang et al., 2009). Meanwhile, GA was found mainly excreted through bile as unchanged form after i.v. administration, while only traces of GA (1.04 %) appeared in the feces and no GA was detected in rat urine (Hao et al., 2007a). The excretion data suggested that a great amount of GA was metabolized extensively in the intestine of rats. However, there is little documented information about the intestinal metabolism of GA either in animals or humans to the best of our knowledge. Considering the efficacy and safety of GA injection, the current study is thus dedicated to clarify the final disposition and metabolic profile of GA in rats. Interestedly, a rare intestinal metabolic pathway responsible for the final disposition of GA in rats is revealed. Moreover, comparing to the previous metabolic studies of GA, a more integrated metabolic profile in rats is proposed according to the results of *in vitro* and *in vivo* studies. Besides, since the the main pharmacophore of GA, the 9, 10 carbon-carbon double bond (Zhang et al., 2004; Palempalli et al., 2009), is also the metabolic soft spot of this molecule, the implication of the metabolism for the anti-tumor effect of GA is further discussed.

Materials and Methods

Materials GA reference standard (99.3% purity) and the GA injection containing 20 mg of GA per vial, which was provided by Jiangsu Kanion Pharmaceutical Co., Ltd. (Lianyungang, China). 10-hydroxygambogic acid (M11) was prepared as our previous reported method (Yang et al., 2010b). NADPH, UDPGA, reduced glutathione, alamethicin, saccharic acid-1, 4-lactone, Tris-base, β-glucuronidase (EC 3.2.1.31, from *Escherichia coli*) and β-glucosidase (EC 3.2.1.21, from *almonds*) were purchased from Sigma-Aldrich (St. Louis, MO). $NaHSO_3$, NaOH, ethyl acetate, ammonium acetate and alcohol were all analytical grade and obtained from Sinopharm Chemical Reagent Co, Ltd. (SCRC) (Shanghai, China). Rat liver microsomes (RLMs) used in this study were purchased by the Research Institute for Liver Disease Co. (RILD) (Shanghai, China). The microsomes had been previously characterized for CYP1A2, CYP2C6, CYP2C11, CYP2D2, and CYP3A1/2 activities by RILD. PBS was also kindly provided by RILD. HPLC grade acetonitrile and methanol were obtained from Tedia (Fairfield, USA). HPLC grade acetic acid was obtained from Fisher scientific (Shanghai, China). Deionized water was purified using a Milli-Q system (Millipore, Milford, MA, USA).

Chemical Syntheses

Synthesis and isolation of 10-α SGA (M21, Reference)and 10-β SGA (M22, Reference) GA (500 mg, 0.8 mmol) was dissolved in ethanol (50 mL) and added dropwise to a clear solution of $NaHSO_3$ (500 mg, 5 mmol in 10 mL water) at room temperature. After being stirred at 50 °C for about 8 h, the reaction mixture was extracted with ethyl acetate. Then, the organic phase was collected and evaporated to dryness and then the residue was dissolved in 100 mL mobile phase. The reconstituted

DMD Fast Forward. Published on December 29, 2010 as DOI: 10.1124/dmd.110.037044
This article has not been copyedited and formatted. The final version may differ from this version.

solution was subjected to P6000^{TM} preparation HPLC (C18, 150 × 40.5 mm i.d.10 μm, ChuangXinTongHeng Science And Technology Co., Ltd, Beijing, China) equipped with A1359 manual sampler and a UV6000 detector (ChuangXinTongHeng Science And Technology Co., Ltd, Beijing, China) with a detection wavelength set at 320 nm. The mobile phase, delivered at a constant flow rate of 10 mL/min, consisted of a gradient of solvent A (methanol) in solvent B (water), as follows: 0 to 10 min, 50 % A; 20 to 38 min, 90 % A. 10-β SGA was collected at the time region of 21-24 min, and 10-α SGA was collected at the time region of 27.5-29 min. 10 injections were made. The eluted sample was collected into the glass vials and evaporated to dryness to give 108 mg of 10-α SGA and 23 mg of 10-β SGA. The purities of 10-α SGA and 10-β SGA were 97.3 % and 96.4 %, respectively, based on HPLC analysis by area normalization method. Identities of the 10-α SGA and 10-β SGA were confirmed by examining the UV, MS and NMR spectra.

Synthesis of 10-GGA (M1 Reference) GA (250 mg, 0.4 mmol) was dissolved in ethanol (20 mL) and added dropwise to a clear solution of reduced glutathione (1000 mg, 3.3 mmol in 50 mL PBS at pH 7.4) at room temperature. After being stirred at 37 ℃ for about 24 h, the reaction mixture was extracted with ethyl acetate. Then, the organic phase was collected and evaporated to dryness and then the residue was dissolved in 50 mL water. The reconstituted solution was also subjected to P6000^{TM} preparation HPLC system with a detection wavelength set at 320 nm. The separation was performed with a mobile phase of methanol-water (90:10, v/v) at flow rate of 10 mL/min, and 10- GGA was collected at the time region of 8.5-12 min. Five injection was made. The eluted samples were collected into the glass vials and evaporated to dryness under N_2, and 197 mg residue of 10-GGA was obtained. The purity of

10-GGA was 93.4 %, which based on HPLC analysis by area normalization method. Identity of the 10-GGA was confirmed by examining the UV, MS and NMR spectra.

Dosing Procedure and Sample Collection The GA injection containing 20 mg of GA per vial was kindly provided by Jiangsu Kanion Pharmaceutical Co., Ltd. (Lianyungang, China). The solution of the GA injection was formulated shortly before administration, and a dosage of 4 mg/kg was delivered in a volume of 2 mL. Sprague Dawley rats (250 ± 20 g) were purchased from the Qinglongshan Experimental Animal Center (Nanjing, China). The animal was housed under standard conditions with food and water provided ad libitum. The animal study was approved by the Animal Ethics Committee of China Pharmaceutical University.

Plasma Collection: Six rats were dosed by intravenous administration via the tail vein. Blood samples (0.1 mL) were collected from the tail vein in 0.25 mL sodium heparinized tubes before and 0.033, 0.067, 0.15, 0.3, 0.75, 1, 2 and 4 h after intravenous administration of GA. Plasma samples were separated by centrifugation for 10 min at 3000 × *g* at 4 °C and pooled over 0 to 4 h.

Bile Collection: Four rats were implanted with a PE-10 cannula into the bile duct under anesthesia by chloral hydrate, and then allowed to recover for 1 h before dosing. Prior to dosing, the bile flow was checked and a pre-dose sample was collected. The bile samples were collected on ice and pooled over 0 to 24 h after the i.v. administration.

Urine and Feces Collection: Rat urine and feces were collected respectively from four rats and pooled over 0 to 24 h after 4 mg/kg i.v. dose of GA via the tail vein.

All the samples mentioned above were stored at -20 °C until use.

NADPH-dependent CYP-mediated and non-CYP-mediated metabolism Incubations with liver microsomes consisted of GA (50 μM), microsomes (1.0 mg/mL), and NADPH (6.0 mM) in 1.0 mL of 0.1 M PBS buffer (pH 7.4). GA in 5.0 μL of acetonitrile was added to the incubation tubes containing buffer and microsomes. After mixing, the tubes were pre-incubated for 10 minutes in a shaking water bath at 37 °C. The reactions were initiated by the addition of 100 μL of 100 mM NADPH solution in water and carried out at 37 °C for 1 h. Control incubations were conducted under the same conditions without NADPH or microsomes. All incubations were performed in duplicate.

UDPGA-dependent UGT-mediated metabolism Incubations with liver microsomes consisted of GA or 10-hydroxygambogic acid (50 μM), microsomes (1.0 mg/mL), saccharic acid-1, 4-lactone (6 mM) and UDPGA (6.0 mM) in 1.0 mL of 0.05 M Tris-HCl buffer (pH 7.4). Alamethicin (50 μg/mg protein) was mixed with liver microsomes for use in incubations. GA or 10-hydroxygambogic acid in 5.0 μL of acetonitrile was added to the incubation tubes containing buffer, alamethicin, saccharic acid-1, 4-lactone and microsomes. After mixing, the tubes were pre-incubated for 10 minutes in a shaking water bath at 37 °C. The reactions were initiated by the addition of 50 μL of 200 mM UDPGA solution in water and carried out at 37 °C for 2 h. Control incubations were conducted under the same conditions without UDPGA or microsomes. All incubations were performed in duplicate.

GSH-dependent non-GST-mediated metabolism Incubations with liver microsomes consisted of GA (50 μM), microsomes (1.0 mg/mL), GSH (5.0 mM) and NADPH (6.0 mM) in 1.0 mL of 0.1 M PBS buffer (pH 7.4). GA in 5.0 μL of

acetonitrile was added to the incubation tubes containing buffer and microsomes. After mixing, the tubes were pre-incubated for 10 minutes in a shaking water bath at 37 ℃. The reactions were initiated by the addition of 100 μL of 100 mM NADPH solution in water and carried out at 37 °C for 2 h. Control incubations were conducted under the same conditions without GSH, NADPH or microsomes, respectively. All incubations were performed in duplicate.

Sample Preparation Aliquot of 1-mL plasma sample was extracted with 4mL ethyl acetate. Following centrifugation and separation, the organic phase was evaporated to dryness under a stream of nitrogen in a water bath of 40 °C. The residue was reconstituted in 150 μL of mobile phase, and a 5 μL aliquot was injected into the LC-MS/MS system. Fecal specimens (0.6 g) were initially homogenized in 4 mL of acetonitrile-water solution (50:50, v/v), and the suspension was centrifuged at 3000*g* for 10 min after the ultrasonic vibration for 10 min. The supernatant was collected and filtered through precut membranes (0.45 μm). The filter was applied to a 10 mL centrifuge tube, and extracted with the same procedures as the plasma sample preparation.

All the incubation reactions were stopped by the addition of 2.0 mL ice-cold acetonitrile. Samples were vortex-mixed. Denatured proteins were separated by centrifugation at 11, 000 *g* and 4 °C for 10 minutes in an Eppendorf 5804 R centrifuge (Hamburg, Germany). The supernatant was transferred and evaporated to dryness under a stream of nitrogen in a water bath of 40 °C. The residue was reconstituted in 150 μL of mobile phase, and a 5 μL aliquot was injected into the LC-MS/MS system.

Hydrolysis Experiments The sample prepared from incubations with rat liver

microsomes in the presence of UDPGA was dried under a nitrogen stream. The residue was reconstituted in 1 mL of 0.1 M Tris buffer, pH 6.8. Approximately 830 units of β-glucuronidase in 100 µL of 0.1 M Tris buffer, pH 6.8, was added to 0.5 mL of the reconstituted solution, and the mixture was incubated at 37 °C for 1 h with gentle shaking. The reaction was stopped by the addition of 1 mL of acetonitrile and the precipitated enzyme was removed by centrifugation. The supernatant was transferred and analyzed by LC-MS/MS. A control incubation was prepared under the same conditions, but without β-glucuronidase. In parallel, 200 µL of the same reconstituted solution were submitted to alkaline hydrolysis by incubation with or without 0.5 M NaOH (10 µL) during 2 h at room temperature. After adjustment with 20 µL 1% acetic acid to about pH 7.0, an aliquot of 5µL was analyzed by LC-MS/MS.

LC-DAD-MS/MS Analysis The HPLC was performed using a Finnigan Surveyor LC Pump with an autosampler (Thermo Finnigan, San Jose, CA, USA). Gradient chromatographic separation was performed on a Luna C18 column (150 × 2.0 mm i.d., 3.0 µm, Phenomenex, Torrance, CA, USA) with a security C18 guard column (4×2.0 mm i.d., Phenomenex, Torrance, CA, USA); For the bile metabolites identification, the mobile phase, delivered at a constant flow rate of 0.25 mL/min, consisted of a gradient of solvent A (acetonitrile) in solvent B (10 mM ammonium acetate in water), as follows: 0 to 19 min, 38 % A; 30 to 45 min, 80 % A; 45.1 to 50 min, 38 % A. For feces metabolites identification, the mobile phase consisted of a gradient of solvent A in solvent B as follows: 0 to 19 min, 38 % A; 25 to 40 min, 80 % A; 40.1 to 45 min, 38 % A. For plasma metabolites identification, isocratic chromatographic separation was performed and the mobile phase consisted of a 68 % A. For *in vitro* phase I metabolites and GSH adduct of GA identification, isocratic chromatographic

separation was performed and the mobile phase consisted of a 65 % A in solvent B. For in vitro glucuronide metabolites identification, the mobile phase consisted of a gradient of solvent A in solvent B as follows: 0 to 2 min, 50 % A; 2 to 8 min, 80 % A; 8.1 to 18 min, 95 % A; 18.1 to 25, 50 % A. The column temperature was maintained at 40 °C. Sample injection volume was 5.0 µL. A TSQ Quantum Discovery MAX triple-quadrupole mass spectrometer (Thermo Finnigan, San Jose, CA, USA), equipped with an electrospray ionization (ESI) source, was used in negative ion mode. The spray voltage was set to 3.0 kV, and the capillary temperature was maintained at 320 °C. Nitrogen was used as the sheath gas (30 Arb) and auxiliary gas (5 Arb) for nebulization. For collision-induced dissociation (CID), argon was used as the collision gas at a pressure of 1.5 mTorr. The collision energy in the in-source CID mode was set at 7 eV. Both Q1 and Q3 peak widths were set at 0.7 Th. The detection wavelength was set at 320 nm, and UV spectra from 200 to 400 nm were also recorded for peak characterization. Analytical data were acquired using Xcalibur software.

NMR Analysis The NMR spectra of the analytes were recorded at 303 K on Bruker ACF-500 NMR spectrometer（500 MHz, Bruker, Faellanden, Switzerland）equipped with a 5 mm probe, using DMSO-d_6 as solvent. Chemical shifts are reported in ppm relative to tetramethylsilane (TMS).

DMD Fast Forward. Published on December 29, 2010 as DOI: 10.1124/dmd.110.037044
This article has not been copyedited and formatted. The final version may differ from this version.

Results

Identification of the rare intestinal metabolites of GA in rats

Previous study of GA suggests that GA is mainly excreted through bile as unchanged form, whereas only traces of GA appeared in the feces (Hao et al., 2007a). It suggests that a great amount of GA is metabolized extensively in the intestine of rats. In order to clarify the final disposition of GA in rats, we first investigated the metabolic profile of GA in rat feces using LC-DAD-MS/MS. Interestingly, we found two abundant GA related peaks which were designated as M21 and M22 with retention time at 16.9 and 19.4 min in the chromatogram, respectively (Fig. 2). The MS spectra of M21 and M22 both exhibited $[M-H]^-$ ions at the same *m/z* 709 in negative ion ESI mode (Fig. 3). The MS/MS analysis showed that the two ions underwent almost the same fragmentation pathways to give the common fragment ions at *m/z* 627, 583, 539 which were identical to the diagnostic fragment ions of GA (Fig. 3). The MS analyses suggested that M21 and M22 might be a pair of isomers and both gave the fragment ions at *m/z* 627, the same m/z value as the deprotonated molecule ion of GA, which resulted from the neutral loss of 82 Da. The UV spectrum of these two metabolites showed that their maximum absorption wavelengths were 275, 320 nm for M21 and 280, 320 nm for M22, respectively (Fig. 3), indicating that the 9, 10-double bond might be absent. Accordingly, a mass shift of 82 Da compared with GA might result from a rare sulfonation metabolic pathway which possibly took place at the α, β-unsaturated ketone structure of GA for the two isomers. The steric configurations of these isomers could be readily distinguished by their stability in the MS ionization source. As shown in the Fig. 3, the relative abundance of the fragment ion at *m/z* 627 of the two isomers were 11.4 % for M21 and 24.7 % for M22. It suggested that the neutral loss of H_2SO_3 (82 Da) was easier to take place in the

structure of the latter than the former under in-source CID. Therefore, H-9 and the sulfonic acid at C-10 of the latter might possess the same configuration because of the well known steric effect. Then, the two isomers of rare sulfonic acid metabolites of GA were synthesized by reacting $NaHSO_3$ with GA and NMR analyses allowed the definitive assignment of their structures as 10-α SGA and 10-β SGA. As shown in Table 1, the chemical shift of H-10 migrated from δ 7.60 ppm (GA) to 3.87 for 10-α SGA and 3.43 ppm for 10-β SGA, respectively, implying that an electron-withdrawing group, most likely the sulfur of sulfonic acid, was introduced to C-10. Similar ^{13}C-NMR chemical shift migration of C-10 from 135.3 ppm (GA) to 42.7 for 10-α SGA and 43.3 ppm for 10-β SGA, respectively, was observed (Table 2). The NMR data on these references of the two isomers strongly indicated that sulfonic acid was conjugated at the C-10 of GA. In order to provide unequivocal elucidation of the steric configurations of these isomers, the NOESY experiment was carried out. As shown in Fig. 4, the NOESY correlations between H-9 and H-10, H-10 and H-21β, H-21β and H22 were observed for 10-α SGA, indicating the H-9, H-10 and the sulfonic acid at C-10 of 10-α SGA were β, β and α configuration, respectively (Jia et al., 2008). Complete proton and carbon chemical shift assignments for the references of 10-α SGA and 10-β SGA were accomplished using the ^{1}H-^{1}H COSY, DEPT, HSQC, HMBC and NOESY NMR spectra and shown in the Table 1 and 2. Since the predominated metabolites (M21/22) found in rat feces showed the same retention time and mass spectra as those of synthetic reference standards (Supplemental Fig. S1), they were finally identified as 10-α sulfonic acid GA and 10-β sulfonic acid GA, respectively.

Then, *in vitro* incubation experiment was conducted to investigate whether this rare sulfonation metabolic pathway was mediated by the SULT in microsomes. However,

no metabolite of GA was founded in such incubation system (Data not shown). It suggested that the rare sulfonation metabolic pathway was not mediated by SULT and might result from Michael addition reaction of GA from biliary excretion with sulfur-containing chemical substance in the intestinal content. In order to validate this hypothesis, we attempted to incubate the intestinal contents with GA (Refer to the Supplemental data). As expected, the two sulfonic acid conjugates were found in such incubation system (Supplemental Fig.S2).

Identification of other metabolites of GA in rats

M0 (Parent drug)

M0 was found in the plasma, bile and feces. Upon the negative ion ESI-MS full scan mode, the M0 showed the abundant deprotonated molecule ion at *m/z* 627. The product ion scanning spectrum of this ion provided the characteristic fragment ions at *m/z* 583, 539, 459 and 353 which were identical to those of GA (Table 3). It was therefore identified as GA, the parent drug, further confirmed by comparison of its retention time on LC-MS with the standard reference substance.

M1 (Glutathionyl conjugation)

M1 was found in the bile (Fig. 5). The MS spectrum of metabolite M1 exhibited $[M-H]^-$ ions at *m/z* 934 in negative ion ESI mode (Fig. 6). The MS/MS analysis showed a main fragment ion at *m/z* 306 $[M-H-628]^-$ resulting from neutral loss of its parent drug, GA, due to cleavage between cysteinyl C-S bond (Fig. 6), and some other fragment ions resulting from the successive loss of H_2O, H_2S and cleavage of amide linkage, especially the usual diagnostic fragment ion of GSH adducts in the negative ion mode, the ion at *m/z* 272 (Tang and Lu, 2010). Meanwhile, the characterized

DMD Fast Forward. Published on December 29, 2010 as DOI: 10.1124/dmd.110.037044
This article has not been copyedited and formatted. The final version may differ from this version.

neutral loss of pyroglutamate (129 Da) (Levsen et al., 2005) was observed in the positive ion ESI-MS/MS experiment (Supplemental Fig. S3). All of these results suggested that M1 might contain a GSH moiety. The UV spectrum of M1 showed that the maximum absorptions at 275 and 320 nm, preliminarily indicating that the 9, 10-double bond might be absent and GSH was conjugated at the C-10 of GA (Feng et al., 2007; Yang et al., 2010b). Then, the GSH adduct of GA reference was synthesized as the method mentioned above, and NMR analyses allowed the unequivocal assignment of the structure. As shown in Table 1, the chemical shift of H-10 migrated from δ 7.60 ppm (GA) to 3.96 ppm, implying that an electron-withdrawing group, most likely the sulfur of GSH, was introduced to C-10. Similar chemical shift migration of C-10 from 135.3 ppm (GA) to 38.1 ppm was observed in the ^{13}C-NMR spectra of GA and its GSH adducts (Table 2). The presence of glutathionyl moiety was confirmed by the diagnostic proton signals for the GSH moiety in the region from 1.8 to 4.5 ppm (Table 1 and Supplemental Fig. S4) (Kang et al., 2008; Shimizu et al., 2009; Wang et al., 2009). Moreover, the ^{13}C-NMR spectrum (Table 2 and Supplemental Fig. S4) also showed the expected signals for the GSH moiety (C-α-Glu, C-α-Cys, C-α-Gly, C-γ-Glu, C-β-Cys, and C-β-Glu). Complete proton and carbon chemical shift assignments were accomplished using the ^{1}H-^{1}H COSY, DEPT and HSQC NMR spectra. These UV, MS and NMR data on this synthesized reference substance unequivocally indicated that GSH was conjugated at the C-10 of GA. Due to the retention time and spectral data of the M1 in rat bile were consistent with those of GSH adduct of GA , it was finally identified as 10-GGA.

In vitro experiment was then conducted to investigate whether the formation of this metabolite was mediated by GSH-dependent GST in the RLMs. Interestingly, M1 peak appeared in the incubation system in the presence of GSH whether there was

microsome or not (Data not shown), suggesting that the formation of M1 was not mediated by GST enzyme in the RLMs.

M2, M3, M5, M8 and M13 (Mono-oxidation)

M2, M3, M5 and M8 were found in the rat bile. MS analysis showed that their deprotonated molecule ions $[M-H]^-$ all at *m/z* 643 which was 16 Da larger than the deprotonated molecular ion for GA, indicating that they might be the mono-oxidation products of GA. UV analysis showed that the maximum absorption of all these metabolites at 290, 360 nm, indicating that the conjugated π–electron system might retain. These findings suggested oxidation might take place at the side chains. The product ion scan spectra of these deprotonated molecule ions showed a common characteristic fragment ion at *m/z* 475 which was 16 Da larger than the diagnostic fragment ion of GA at *m/z* 459 resulting from the RDA rearrangement and continuing loss of substituted side chain at C-13 (Supplemental Fig. S5A), indicating that mono-oxidations probably took place at the other two side chain, the prenyl unit at C-17 and the geranyl unit at C-2. However, we failed to assign the exact substitution due to the lack of NMR data and further study was needed.

M13 was found in the rat bile and feces. MS analysis showed that its deprotonated molecule ion $[M-H]^-$ at *m/z* 643 which was 16 Da larger than the deprotonated molecular ion for GA. The product ion scan spectrum of *m/z* 643 showed that the major fragment ions at *m/z* 559, 543, 527, 485, 481, 447, 443, 373, 325, 285. Moreover, UV analysis showed that the maximum absorptions of this metabolite at 275, 335 nm. All of these spectral data and chromatographic behavior were identical to that of 9, 10-epoxylGA reported in the literatures (Feng et al., 2007; Zhang et al., 2009), M13 was thus identified as 9, 10-epoxylGA.

As shown in the Fig. 7, all these mono-oxidation products of GA appeared in the microsome incubation system in the presence of NADPH, while no metabolites were found in the control test, suggesting that the formation of all these mono-oxidation product of GA was mediated by NADPH-dependent CYP enzyme in the rats liver microsome.

M4, M11 (Hydration)

M11 was found in the plasma (Supplemental Fig. S6), bile and feces. MS analysis showed that its deprotonated molecule ion $[M-H]^-$ at *m/z* 645 which was 18 Da larger than the deprotonated molecular ion for GA. The product ion scan spectrum of *m/z* 645 showed that the major fragment ions at *m/z* 627, 583 and 539. Moreover, UV analysis showed that the maximum absorptions of this metabolite at 275, 320 nm. All of these results suggested that this metabolite might be 10-OHGA. It was further confirmed by comparison of its retention time on LC-MS with the standard reference substance. This finding suggested that M11 was also the major circulating metabolite of GA in rats, which was similar to that observed for humans (Yang et al., 2010b), indicating that the safety evaluation using this species in a preclinical setting was reasonable.

M4 was found in the bile. MS analysis showed that its deprotonated molecule ion $[M-H]^-$ at *m/z* 645 which was 18 Da larger than the deprotonated molecular ion for GA. Different from M11, UV analysis showed that the maximum absorptions of this metabolite at 290, 360 nm, indicating that the conjugated π-electron system might retain. These findings suggested the metabolism might take place at the side chains. The product ion scan spectrum of *m/z* 645 showed that the major fragment ions at *m/z* 611, 557, 459, 445 and 401. The ions at *m/z* 611 and 557 were the products of

successive loss of CO_2 from the $[M-H]^-$ of M4. Interestingly, the ions at *m/z* 459 and 445 were as same as the diagnostic fragment ion of GA resulting from the RDA rearrangement and continuing loss of prenyl unit (Supplemental Fig. S5B), indicating the hydration might take place at the C13 side chain. Therefore, it is reasonable to assume that the most possible hydration part is C27-C28 double bond.

In vitro experiment was then conducted to investigate whether the formation of these two hydrate metabolites was mediated by NADPH-dependent CYP. As shown in the Fig. 7A, both hydrate metabolites were formed in the microsome incubation system in the presence of NADPH. No metabolites were found in the incubation system which was absence of both microsome and NADPH (Fig. 7B). Interestingly, M11 peak appeared whether there was microsome or not, while M4 could only form in the microsome incubation system (Fig. 7C). Moreover, stability study showed that GA was stable in the 0.1 M PBS buffer (pH 7.4) during the incubation time (Data not shown). These findings suggested that M4 was metabolized by NADPH-dependent CYP enzyme in the rats liver microsome, while M11 was not.

Apparently, NADPH can not directly react with GA. Thus, it may catalyze the hydration of GA via some indirect procedures. Since NADPH in H_2O could be successively consumed under air (O_2) and produce $O_2^{-\cdot}$ and H_2O_2, we investigated the effect of condition without O_2 on the formation of M11. Interestedly, the formation of M11 was greatly inhibited by expelling air with a gentle N_2 stream (Supplemental Fig. S7). Meanwhile, NADPH increased the formation of M11 in a dose-dependent manner. These results suggested that hydration of GA might be catalyzed by $O_2^{-\cdot}$ or H_2O_2 which was generated by the reaction of NADPH with O_2 in the air.

M6, M7 (Glucuronidation)

M6 and M7 were found in both bile and feces samples (Fig. 2 and 5). The identity of M7 was elucidated by UV and MS spectra and further confirmed by *in vitro* study and hydrolysis experiment. The UV spectrum of M7 showed that the maximum absorptions at 290, 360 nm which were identical to those of GA. MS analysis showed that M7 had a deprotonated molecular ion at *m/z* 803. The supplemental Fig. S8 shows the product ions of *m/z* 803 obtained from CID. Loss of a moiety of 176 Da generated the same ion as the deprotonated molecular ion of GA, indicating that M7 might be the GA glucuronide. The ions at *m/z* 583, 539, and 459 were the same fragmentation products as those of GA. Then, *in vitro* study was carried out to confirm this finding. After incubation with rats liver microsomes in the presence of UDPGA, GA was partly metabolized to a glucuronide peak with the same spectral behavior of M7 (Fig. 8). After hydrolysis with β-glucuronidase for 1 h, the glucuronide peak formed *in vitro* dramatically decreased (Supplemental Fig. S9). After hydrolysis under alkaline conditions for 2 h, the glucuronide peaks completely disappeared (Supplemental Fig. S9), indicating that this glucuronide was labile under alkaline conditions. These findings strongly suggested that the glucuronide was an acyl glucuronide of GA rather than the phenolic glucuronide of GA (Tong et al., 2007).

M6 was identified with the similar procedures to M7. The UV spectrum of M7 showed that the maximum absorptions at 275, 320 nm which were identical to those of M11. The deprotonated molecular ion for M6 was observed at *m/z* 821 which was 176 Da larger than the deprotonated molecular ion for M11. Neutral loss of 176 Da from the deprotonated molecular ion of M6 produced the ion at *m/z* 645, identical to M11 deprotonated molecular ion, indicating that the metabolite might be the M11

glucuronides (Supplemental Fig. S8). Similar to M7 described above, the M6 formed *in vitro* was not only hydrolyzed by β-glucuronidase but also hydrolyzed under alkaline conditions (Supplemental Fig. S9). These findings suggested that the glucuronide was an acyl glucuronide of M11.

M9, M10, M12 (Glucosidation)

M9, M10 and M12 were found in both bile samples. The identities of these metabolites were elucidated by UV and MS spectra. The UV spectra of M9, M10 and M12 were similar with those of M11, M13 and GA, respectively (Table 3). The MS analyses showed that M9, M10 and M12 had deprotonated molecular ions at *m/z* 807, 805 and 789, respectively (Fig. 9), which were 162 Da larger than the deprotonated molecular ions for M11, M13 and GA, respectively. Characteristic neutral loss of 162 Da (Levsen et al., 2005) from the deprotonated molecular ions of M9, M10 and M12 produced the ions at *m/z* 645, 643 and 627 identical to the deprotonated molecular ions of M11, M13 and GA, respectively (Fig. 9), indicating that the metabolite might be the glucosides of M11, M13 and GA, respectively.

Discussion

According to much researches over the last decade, it can be realized that the intestine play a major role in the metabolism and disposition of xenobiotics, especially the natural products (Fisher and Labissiere, 2007; Bi et al., 2010). Generally, the intestinal metabolism of xenobiotics is mainly catalyzed by the cytochrome P450 superfamily and/or the conjugating enzymes such as UGT, SULT and GST in the intestinal mucosal cells (Kaminsky and Zhang, 2003; Zhang et al., 2007). In addition to these common Phase I and II metabolism, there are other metabolic pathways in the intestinal tract which are mainly mediated by intestinal flora, especially the rare ones such as isomerization, cleavage of a carbon-carbon bond, and polymerization (Yang et al., 2003).

In this study, a high amount of rare sulfonic acid metabolites of GA, a pair of isomers, were originally found in the rats' fecal samples after administration, while these two isomers were not detected in the biliary samples, suggesting that the sulfonic acid metabolites were produced abundantly in the intestinal tract of rats. Since GA is found mainly excreted into intestinal tract through bile in rats after dose, this rare intestinal metabolism may be responsible for the final disposition of GA in rats. The sulfonic acid metabolites are rare, but they are also found in the metabolic studies of *N*-[4-chloro-2-fluoro-5-[(1-methyl-2-propynyl)oxy]phenyl]-3, 4, 5, 6-tetrahydrophthalimide (S-23121) (Yoshino et al., 1993), andrographolide (He et al., 2003) and menthofuran (Chen et al., 2003) in rats. Interestingly, all these compounds or their metabolic intermediate contain the functional group in which the olefins or acetylenes conjugated to electron-withdrawing groups, or the so-called Michael reaction acceptors, such as unsaturated ketoaldehyde. These studies have indicated that the mechanism of biosynthesis of the sulfonic acid conjugates involves direct

addition of sulfite ion to the α, β-unsaturated ketone, likely by the gut flora (Yoshino et al., 1993; Chen et al., 2003). The action of gut flora was not to catalyze the sulfonation directly but to transform inorganic sulfate to sulfite. Other studies reported that the generation of sulfite is probably driven by the successive oxidation of dietary components such as sulfur-containing amino acids (Coloso and Stipanuk, 1989) and/or the reduction of inorganic sulfate by gut flora (Beerens and Romond, 1977; Willis et al., 1997). Additionally, sulfites are usually added to food as preservative antioxidants, bleaching agents, or dough conditioning agents (Rodriguez Vieytes et al., 1994). Therefore, the sulfites in the intestinal tract can be also derived directly from food intake. In this study, the two sulfonic acid conjugates were not only found in the fecal samples after dose, but also formed when GA was incubated with the contents in the rat gut. These results suggested that the sulfonation of GA in the rat intestine might also result from the direct addition of sulfite ion to the 9, 10 carbon-carbon double bond of GA (Fig.10). Another possible mechanism involves addition of glutathione to the unsaturated ketoaldehyde followed by further metabolism to give the sulfonic acid conjugates (Chen et al., 2003; Levsen et al., 2005). However, only a small amount of GSH adducts of GA was found in the rats bile (Fig. 5), indicating that most sulfonic acid conjugates were not the degradation products of 10-glutathionyl GA (M1). Therefore, the Michael addition reaction between GA from biliary excretion and the sulfite in the intestinal content may be the dominant mechanism of the biosynthesis of the sulfonic acid conjugates of GA. These results provides information on the major metabolic soft spot of GA in the intestine of rats which is not only useful in further metabolic study of this molecule in humans, but also helpful for better understanding the efficacy and safety of GA injection which is now under a phase II clinical trial in China. Moreover, it is also of value in the

metabolic studies of other cytotoxic caged xanthones from gamboge (Jia et al., 2008; Han and Xu, 2009; Tao et al., 2009; Li et al., 2010) and chemically synthetic anti-tumor candidates using GA as the leading compounds, such as gambogic amide (Jang et al., 2007) and *N*-(carboxymethyl)-gambogamide (Xie et al., 2009).

It has been well demonstrated that Michael reaction acceptor molecules can covalently modify some biological nucleophiles such as DNA and proteins and whereby directly or indirectly involve in the cell cycle and life processes (Zhao and Cong, 2007). As expected, the structure–activity relationship studies show that derivatives of GA without the 9,10 carbon–carbon double bond in the α, β-unsaturated ketone are found to be inactive in the caspase activation assay in cancer cell lines tested at concentrations up to 10 mM, and these compounds are more than 10-fold less active than GA in such cells (Zhang et al., 2004). A recent study suggests that GA strongly blocked the activation of NF-κB induced by lipopolysaccharide, whereas 9,10-dihydro-GA, which lacks the reactive α, β-unsaturated carbonyl group, is ineffective, and *in vitro* kinase assays coupled with interaction studies using biotinylated GA as well as proteomic analysis demonstrate that inhibitory κB kinase β, a key kinase of the NF-κB signaling axis, is covalently modified by GA at Cys-179, causing significant inhibition of its kinase activity (Palempalli et al., 2009). Taken together, the 9,10 carbon–carbon double bond of the α, β-unsaturated ketone is critial for the anti-cancer activity of GA. However, this study reveals that 9,10 carbon–carbon double bond is also the metabolic soft spot of the molecule by sulfonation (M21/22), glutathionylation (M1), hydration (M11) and epoxidation (M13). Although the anticancer activities of these major metabolites without 9,10 carbon–carbon double bond have not been tested in this study, it is proper to presume that they are much less active than their parent drug or even ineffective. On the other

hand, *in vitro* study suggested that GA rapidly covalently conjugated with GSH, while only a little amount of GSH adduct of GA (M1, 10-glutathionyl GA) was found in the biliary samples of rats (Fig. 5). A recent work finds that glutathionylation represents a key cellular metabolic event in the regulation of the anti-inflammatory and anticancer activities of GA (Palempalli et al., 2009). Thus, it can be hypothesized that if *in vivo* reversibility of GSH adduct of GA could occur, it could represent a mechanism for GA delivering and regenerating to the pharmacological target. Further investigation is needed to obtain an in-depth understanding of the mechanism and its impact on the anticancer activity of this compound.

Besides, this study provides a more integrated metabolic profile in the liver of rats comparing to the previous reports about the metabolism of GA, whereas no metabolites or its parent drug are detected in the urine samples which is consistent with previous reports (Hao et al., 2005; Hao et al., 2007a). Several mono-oxidation products of GA metabolized by NADPH dependent CYP450 were detected and their structures were preliminarily analyzed using LC-DAD-MS/MS. A new acyl glucuronide of GA was observed for the first time, while the acyl glucuronide of 9, 10-epoxyGA reported in the literature was not detected in the rat biliary samples. Whether the latter finding is a result of limited acyl glucuronide-conjugation, fast acyl glucuronide-conjugate excretion or degradation, or limitations of the analytical capacity of the instrument, remains to be elucidated. Another newly found phase II metabolic pathway of GA in rats was the conjugation of GA and its metabolites with glucose, which was frequently observed during the biotransformation of xenobiotics in plants while it was relatively rare in mammalian species (Levsen et al., 2005). Nevertheless, the glucosidation has still been observed in the animal metabolic studies of verapamil (Walles et al., 2003), mycophenolic acid (Picard et al., 2005) and

baicalin (Xing, 2005). The mechanism of these conversion and specific enzymes involved are yet unknown and will be examined in the future.

In summary, although GA is metabolized by a variety of routes, including mono-oxidation, hydration, glutathionylation, glucuronidation, glucosidation, in the liver of rats, a large amount of GA is excreted into intestinal tract through bile as unchanged form. The bile excretion process is primarily responsible for removing GA from the systemic circulation and, therefore, responsible for terminating its antitumor effect. A rare intestinal metabolic pathway is responsible for the final disposition of GA in rats and it mainly involves Michael addition of sulfite ion to the 9, 10 carbon-carbon double bond of α, β-unsaturated ketone (Fig. 10). In particular, such metabolites without 9, 10 carbon-carbon double bond, the major pharmacophore of GA, may be much less active than their parent drug or even ineffective.

Acknowledgement

The authors would like to thank Yin-guang Zhang from Department of Medicinal Chemistry of China Pharmaceutical University for his help on chemical syntheses, Dong-jun Chen from Center for Instrumental Analysis, China Pharmaceutical University for his help on NMR analyses, and Dr. Zhuo-han Hu and Dr. Yu-chang Mao from RILD Co. for their helpful discussion on the rat liver microsome incubation experiments. The LC-DAD-MS/MS analyses of this study were conducted in Kanion Pharmaceutical Co., Ltd.

Authorship Contributions

Participated in research design: J.Y., L.D., and S.J.

Conducted experiments: J.Y., L.H., W.Q, X.S., Z.W., and W.X.

Performed data analysis: J.Y., L.H., and L.D.

Wrote or contributed to the writing of the manuscript: J.Y., L.H., and L.D.

Other: L.D. acquired funding for the research

References

Beerens H and Romond C (1977) Sulfate-reducing anaerobic bacteria in human feces. *Am J Clin Nutr* **30:**1770-1776.

Bi X, Du Q and Di L (2010) [Important application of intestinal transporters and metabolism enzymes on gastrointestinal disposal of active ingredients of Chinese materia medica]. *Zhongguo Zhong Yao Za Zhi* **35:**397-400.

Castro-Perez JM (2007) Current and future trends in the application of HPLC-MS to metabolite-identification studies. *Drug Discov Today* **12:**249-256.

Chen LJ, Lebetkin EH and Burka LT (2003) Metabolism of (R)-(+)-menthofuran in Fischer-344 rats: identification of sulfonic acid metabolites. *Drug Metab Dispos* **31:**1208-1213.

Coloso RM and Stipanuk MH (1989) Metabolism of cyst(e)ine in rat enterocytes. *J Nutr* **119:**1914-1924.

Ding L, Huang D, Wang J and Li S (2007) Determination of gambogic acid in human plasma by liquid chromatography-atmospheric pressure chemical ionization-mass spectrometry. *J Chromatogr B Analyt Technol Biomed Life Sci* **846:**112-118.

Feng F, Liu W, Wang Y, Guo Q and You Q (2007) Structure elucidation of metabolites of gambogic acid in vivo in rat bile by high-performance liquid chromatography-mass spectrometry and high-performance liquid chromatography-nuclear magnetic resonance. *J Chromatogr B Analyt Technol Biomed Life Sci* **860:**218-226.

Fisher MB and Labissiere G (2007) The role of the intestine in drug metabolism and pharmacokinetics: an industry perspective. *Curr Drug Metab* **8:**694-699.

Han QB and Xu HX (2009) Caged Garcinia xanthones: development since 1937. *Curr*

Med Chem **16:**3775-3796.

Hao K, Liu XQ and Wang GJ (2005) Pharmacokinetic s of gambogic acid in rats. *Journal of China Pharmaceutical University* **36:**338 - 341.

Hao K, Liu XQ, Wang GJ and Zhao XP (2007a) Pharmacokinetics, tissue distribution and excretion of gambogic acid in rats. *Eur J Drug Metab Pharmacokinet* **32:**63-68.

Hao K, Zhao XP, Liu XQ and Wang GJ (2007b) Determination of gambogic acid in dog plasma by high-performance liquid chromatography for a pharmacokinetic study. *Biomed Chromatogr* **21:**279-283.

He X, Li J, Gao H, Qiu F, Hu K, Cui X and Yao X (2003) Identification of a rare sulfonic acid metabolite of andrographolide in rats. *Drug Metab Dispos* **31:**983-985.

Jang SW, Okada M, Sayeed I, Xiao G, Stein D, Jin P and Ye K (2007) Gambogic amide, a selective agonist for TrkA receptor that possesses robust neurotrophic activity, prevents neuronal cell death. *Proc Natl Acad Sci U S A* **104:**16329-16334.

Jia MM, Shou QY, Tan Q and Shen ZW (2008) Chemical constitutes of *Garcinia hanburyi*. *Acta Chimica Sinica* **66:**2513-2517.

Kaminsky LS and Zhang QY (2003) The small intestine as a xenobiotic-metabolizing organ. *Drug Metab Dispos* **31:**1520-1525.

Kang P, Dalvie D, Smith E and Zhou S (2008) Bioactivation of Flutamide Metabolites by Human Liver Microsomes. *Drug Metab Dispos* **36:**1425-1437.

Levsen K, Schiebel HM, Behnke B, Dotzer R, Dreher W, Elend M and Thiele H (2005) Structure elucidation of phase II metabolites by tandem mass spectrometry: an overview. *J Chromatogr A* **1067:**55-72.

Li Q, Cheng H, Zhu G, Yang L, Zhou A, Wang X, Fang N, Xia L, Su J, Wang M, Peng D and Xu Q (2010) Gambogenic acid inhibits proliferation of A549 cells through apoptosis-inducing and cell cycle arresting. *Biol Pharm Bull* **33:**415-420.

Liu YT, Hao K, Liu XQ and Wang GJ (2006) Metabolism and metabolic inhibition of gambogic acid in rat liver microsomes. *Acta Pharmacol Sin* **27:**1253-1258.

Palempalli UD, Gandhi U, Kalantari P, Vunta H, Arner RJ, Narayan V, Ravindran A and Prabhu KS (2009) Gambogic acid covalently modifies IkappaB kinase-beta subunit to mediate suppression of lipopolysaccharide-induced activation of NF-kappaB in macrophages. *Biochem J* **419:**401-409.

Picard N, Ratanasavanh D, Premaud A, Le Meur Y and Marquet P (2005) Identification of the UDP-glucuronosyltransferase isoforms involved in mycophenolic acid phase II metabolism. *Drug Metab Dispos* **33:**139-146.

Qin Y, Meng L, Hu C, Duan W, Zuo Z, Lin L, Zhang X and Ding J (2007) Gambogic acid inhibits the catalytic activity of human topoisomerase IIalpha by binding to its ATPase domain. *Mol Cancer Ther* **6:**2429-2440.

Rodriguez Vieytes M, Martinez-Sapina J, Taboada Montero C and Lamas Aneiros M (1994) Effect of sulfite intake on intestinal enzyme activity in rats. *Gastroenterol Clin Biol* **18:**306-309.

Shimizu S, Atsumi R, Nakazawa T, Fujimaki Y, Sudo K and Okazaki O (2009) Metabolism of ticlopidine in rats: identification of the main biliary metabolite as a glutathione conjugate of ticlopidine S-oxide. *Drug Metab Dispos* **37:**1904-1915.

Tang W and Lu AY (2010) Metabolic bioactivation and drug-related adverse effects: current status and future directions from a pharmaceutical research perspective.

Drug Metab Rev **42:**225-249.

Tao SJ, Guan SH, Wang W, Lu ZQ, Chen GT, Sha N, Yue QX, Liu X and Guo DA (2009) Cytotoxic polyprenylated xanthones from the resin of Garcinia hanburyi. *J Nat Prod* **72:**117-124.

Tong Z, Li H, Goljer I, McConnell O and Chandrasekaran A (2007) In vitro glucuronidation of thyroxine and triiodothyronine by liver microsomes and recombinant human UDP-glucuronosyltransferases. *Drug Metab Dispos* **35:**2203-2210.

Walles M, Thum T, Levsen K and Borlak J (2003) Metabolism of verapamil: 24 new phase I and phase II metabolites identified in cell cultures of rat hepatocytes by liquid chromatography-tandem mass spectrometry. *J Chromatogr B Analyt Technol Biomed Life Sci* **798:**265-274.

Wang Y, Zhong D, Chen X and Zheng J (2009) Identification of quinone methide metabolites of dauricine in human liver microsomes and in rat bile. *Chem Res Toxicol* **22:**824-834.

Willis CL, Cummings JH, Neale G and Gibson GR (1997) Nutritional aspects of dissimilatory sulfate reduction in the human large intestine. *Curr Microbiol* **35:**294-298.

Xie H, Qin YX, Zhou YL, Tong LJ, Lin LP, Geng MY, Duan WH and Ding J (2009) GA3, a new gambogic acid derivative, exhibits potent antitumor activities in vitro via apoptosis-involved mechanisms. *Acta Pharmacol Sin* **30:**346-354.

Xing J (2005) Study on the absorption and metabolism of baicalin in animals, in: *Pharmaceutical analysis*, Shenyang Pharmaceutical Univerisity, Shenyang.

Yang J, Ding L, Hu L, Jin S, Liu W, Wang Z, Xiao W, You Q and Guo Q (2010a) Comparison of electron capture-atmospheric pressure chemical ionization and

electrospray ionization for the analysis of gambogic acid and its main circulating metabolite in dog plasma. *Eur J Mass Spectrom (Chichester, Eng)* **16:**605-617.

Yang J, Ding L, Jin S, Liu X, Liu W and Wang Z (2010b) Identification and quantitative determination of a major circulating metabolite of gambogic acid in human. *J Chromatogr B Analyt Technol Biomed Life Sci* **878:**659-666.

Yang XW, Hao MR and Masao. H (2003) *Metabolite analysis for chemical consitituents of traditional Chinese medicines*. China Medical Science and Technology Press, Beijing.

Yoshino H, Matsunaga H, Kaneko H, Yoshitake A, Nakatsuka I and Yamada H (1993) Metabolism of N-[4-chloro-2-fluoro-5-[(1-methyl-2-propynl)oxy]phenyl]-3,4,5,6-tetrahydrophthalimide (S-23121) in the rat: I. Identification of a new, sulphonic acid type of conjugate. *Xenobiotica* **23:**609-619.

Zhang HZ, Kasibhatla S, Wang Y, Herich J, Guastella J, Tseng B, Drewe J and Cai SX (2004) Discovery, characterization and SAR of gambogic acid as a potent apoptosis inducer by a HTS assay. *Bioorg Med Chem* **12:**309-317.

Zhang L, You Q, Liang Y, Liu W, Guo Q and Wang J (2009) Identification of gambogic acid metabolites in rat bile by liquid chromatography-tandem mass spectrometry-ion trap-time-of-flight. *Chin J Nat Med* **7:**376-380.

Zhang QY, Kaminsky LS, Dunbar D, Zhang J and Ding X (2007) Role of small intestinal cytochromes p450 in the bioavailability of oral nifedipine. *Drug Metab Dispos* **35:**1617-1623.

Zhao QS and Cong YW (2007) Michael reaction acceptor molecules in chemical biology. *Progress in Chemistry* **19:**1972-1976.

Footnotes:

This work was financially supported by the National Natural Science Foundation of China [Grant 81072609].

The reprint requests should be sent to *prof* Li Ding, Ph.D. Department of Pharmaceutical Analysis, China Pharmaceutical University, 24 Tongjiaxiang, Nanjing 210009, China.Tel: +86 25 83271289, Fax: +86 25 83271289, E-mail: dinglidl@hotmail.com

DMD Fast Forward. Published on December 29, 2010 as DOI: 10.1124/dmd.110.037044
This article has not been copyedited and formatted. The final version may differ from this version.

Legends of Figures:

Fig. 1 Structure of gambogic acid

Fig. 2 Typical chromatograms of blank rat feces (A) and a fecal sample during 0-24 h after an i.v. dose of 4mg/kg of GA in rats (B)

Fig. 3 Proposed fragmentation pathway of sulfonic acid metabolites of GA (A) and the Q1 full scan spectra of M21 (B) and M22 (C) and their product ion scanning spectra (D and E) in the negative ion ESI mode; UV spectra of M21 (F) and M22 (G).

Fig. 4 Expanded region of the chemical shifts exhibiting the key steric ^{1}H-^{1}H correlation (A) in the NOESY spectrum (B) of 10-α SGA (M21 reference) in DMSO-d_6.

Fig. 5 Typical chromatograms of blank rat bile (A) and a biliary sample during 0-24 h after an i.v. dose of 4mg/kg of GA in rats (B)

Fig. 6 Proposed fragmentation pathway of M1 (A) and its product ion scanning spectrum (B) in the negative ion ESI mode. (Inset) the Q1 full scan spectrum of M1

Fig. 7 Typical chromatograms for GA and its metabolites from a variety of *in vitro* incubations: (A) rat liver microsomes in the presence of NADPH; (B) control without NADPH; and (C) control without microsomes

Fig. 8 Typical chromatograms for GA (A) and its acyl glucuronide from a variety of *in vitro* incubations and those for M11 (B).

Fig. 9 The product ion scanning spectra of M12 (A), M10 (B), and M9 (C) in the negative ion ESI mode. Inset: the Q1 full scan spectra of these metabolites.

Fig. 10 The major metabolic pathways of GA in the liver of rats (A) and the proposed mechanism of the final disposition of GA in rats and an implication for the *in vivo* anticancer effect of this natural compound (B).

Table 1. ^{1}H-NMR data of GA and the synthesized reference substances of metabolites (δ in ppm, *J* in Hz)

No.	10-GGA	10-α SGA	10-β SGA	GA
3	5.64 (d, 10)	5.53 (d, 17)	5.62 (d, 10)	5.59 (d, 10)
4	6.57 (d, 10)	6.47 (d, 17)	6.57 (d, 10)	6.55 (d, 10)
6-OH	11.89 (brs)	11.69 (s)	11.93 (s)	12.98 (s)
9	3.71-3.76*	3.10 (d, 12)	3.56 (t, 3)	
10	3.96 (s)	3.87 (d, 12)	3.43 (d, 3.5)	7.60 (d, 7)
11	2.51 (d, 3)	2.64-2.70*	2.65 (dd, 4, 3)	3.49 (dd, 7, 4.5)
19	1.31 (s)	1.38 (s)	1.34 (s)	1.51 (s)
20	1.69 (m)	1.69 (m)	1.64-1.70*	1.69 (m)
21	2.03 (m)*;	3.13 (m);	1.92 (dd, 5.5, 5);	2.24 (dd, 5, 5);
	1.49 (t)*	1.68 (m)	1.39 (dd, 5.5, 5)	1.36 (m)
22	2.54 (d, 8.5)	2.81 (d, 7)	2.46 (d, 7.5)	2.64 (d, 9.5)
24	1.02 (s)	1.11(s)	0.98 (s)	1.18 (s)
25	1.27 (s)	1.61 (s)	1.21 (s)	1.39 (s)
26	3.30 (d, 10);	2.64-2.70*;	3.29 (d, 6.5);	2.83 (dd, 7, 7)
	3.11(d, 10)	2.59 (d, 12.5)	3.17 (d, 3.5)	
27	6.48 (t, 5.5)	5.94 (t, 5.5)	6.61 (t, 5.5)	5.93 (t, 6.5)
29	1.85 (s)	1.45 (s)	1.81 (s)	1.70 (s)
31	3.26 (m);	3.25 (m);	3.24 (dd, 8, 8);	3.27 (dd, 6.5, 8.5);
	3.06 (m)*	3.06 (m)	3.11 (dd, 5.5, 5)	3.10 (m)
32	4.99 (t, 5)	5.22 (t, 10)	5.03 (t, 7)	5.06 (t, 7)*
34	1.72 (s)	1.71 (s)	1.68 (s)	1.61 (s)
35	1.62 (s)*	1.60 (s)	1.60 (s)*	1.60 (s)*
36	2.03 (t, 7)	1.97 (m)	2.02 (dd, 5.5, 6)	1.97 (dd, 8, 8)
37	5.10 (t, 7)	5.04 (t, 10)	5.09 (t, 7)	5.06 (t, 7)*
39	1.62 (s)*	1.64 (s) *	1.60 (s)*	1.60 (s)*
40	1.51 (s)	1.49 (s)	1.50 (s)	1.58 (s)
α-Gly	3.66-3.76*			
α-Glu	3.44 (t, 6.5)			
β-Glu	1.95 (t, 8)			
γ-Glu	2.35 (m)			
α-Cys	4.35 (m)			
β-Cys	3.06*;			
	2.70(t, 11.5)			

***Note**: s, singlet; d, doublet; d, double doublet; t, tripletm, multiplet; brs, broad singlet; *: overlapped signals*

DMD Fast Forward. Published on December 29, 2010 as DOI: 10.1124/dmd.110.037044
This article has not been copyedited and formatted. The final version may differ from this version.

Table 2. ^{13}C-NMR data of GA and the synthesized reference substances of metabolites (δ in ppm)

No.	10-GGA	10-α SGA	10-β SGA	GA
2	81.2	80.7	81.1	81.4
3	126.3	124.6	126.1	125.5
4	115.7	115.6	115.8	115.7
5	101.8	101.4	101.8	102.2
6	155.7	154.5	155.4	157.8
7	102.5	101.4	102.3	100.4
8	195.1	193.6	195.0	179.6
9	48.5	50.3	55.86	132.8
10	38.1	42.7	43.3*	135.3
11	44.0	49.7	41.4	47.0
12	209.2	208.7	209.3	203.7
13	86.3	85.5	87.0	83.3
14	89.6	89.1	89.5	91.4
16	156.0	156.9	156.0	157.1
17	108.2	106.2	107.9	107.3
18	160.6	159.3	160.3	160.9
19	27.0	27.7	27.0	27.6
20	41.4	41.4	41.5	41.7
21	24.5	16.9	23.9	25.0
22	43.3	43.1	43.3*	48.8
23	82.1	81.9	81.5	83.8
24	27.4	27.8	27.3	29.0
25	29.6	29.6	29.8	30.0
26	28.3	28.6	28.9	29.2
27	136.9	135.6	138.9	137.3
28	127.6	126.9	126.5	128.2
29	21.2	20.5	21.2	21.2
30	170.0	167.9	169.2	168.4
31	21.6	21.4	21.6	21.7
32	122.7	122.1	122.7	122.7
33	131.1	130.7	131.0	131.1
34	18.3	17.9	18.2	18.2
35	25.9*	25.6	25.9	25.8
36	22.9	22.4	22.8	22.8
37	124.3	123.9	124.3	124.2
38	132.7	131.1	131.5	131.8
39	25.9*	25.5	25.9	25.8
40	17.8	17.5	17.8	17.8
α-Gly	41.7			
α-Glu	53.6			
β-Glu	27.1			
γ-Glu	31.7			
α-Cys	51.9			
β-Cys	32.8			

***Note**: *: overlapped signals*

DMD Fast Forward. Published on December 29, 2010 as DOI: 10.1124/dmd.110.037044
This article has not been copyedited and formatted. The final version may differ from this version.

Table 3. LC-DAD-MS/MS analysis of GA and its observed metabolites in rat bile samples

No.	t_r (min)	A_{max} (nm)	$[M-H]^-$	Major fragment ions of $[M-H]^-$	Identity
M0	44.8	290, 360	627	583(100), 539, 459, 353	GA [a, b]
M1	5.7	275, 320	934	306(100), 288, 272, 254, 179, 143	10-glutathionyl GA [c]
M2	14.2	290, 360	643	599, 555, 475, 471, 392, 391, 369, 347(100), 337, 285	Hydroxylation of GA [c]
M3	15.7	290, 360	643	599, 555, 475(100), 435, 387, 383, 369, 347, 327	Hydroxylation of GA [c]
M4	18.7	290, 360	645	601(100), 557, 459, 445, 401	Hydration of GA [c]
M5	19.6	290, 360	643	599, 555, 475, 471, 431, 415, 391, 387(100), 347, 287	Hydroxylation of GA [c]
M6	21.3	275, 320	821	803, 645, 627, 583(100), 539, 459, 175	Glucuronide of 10-OHGA [b, c]
M7	23.6	290, 360	803	759, 627, 583(100), 539, 459, 175	Glucuronide of GA [c]
M8	30.2	290, 360	643	599, 555, 537, 475(100), 471, 453, 441, 401, 371, 361	Hydroxylation of GA [c]
M9	38.7	275, 320	807	789, 757(100), 627, 583, 387	Glucoside of 10-OHGA
M10	39.0	275, 335	805	805(100), 643	Glucoside of 9, 10-epoxylGA
M11	39.5	275, 320	645	627, 583(100), 539, 353	10-OHGA [a, b]
M12	40.3	290, 360	789	669, 627, 583(100), 539, 483, 471, 459, 353	Glucoside of GA
M13	43.8	275, 335	643	559, 543, 527, 485, 481, 447(100), 443, 373, 325, 285	9, 10-epoxylGA [b]

***Note**: t_r, retention time; A_{max}: UV maximum absorption wavelength; a, with standard; b, with data in references; c, confirmed by in vitro studies*

Fig. 1

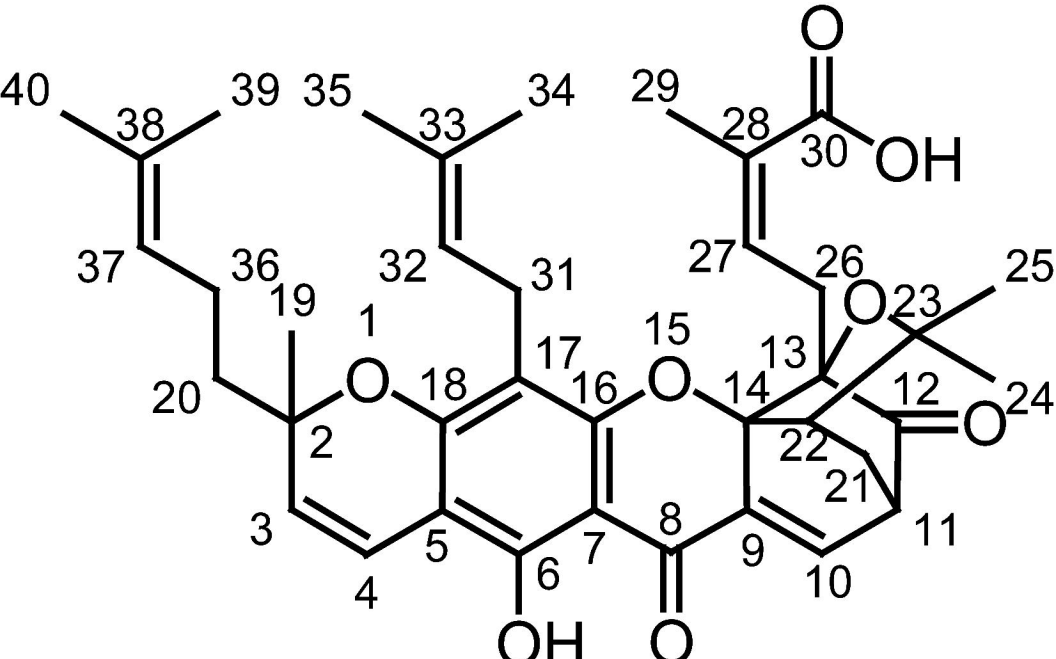
40
38
39
35
33
34
29
28
O
30
OH
37
36
32
31
27
26
25
19
1
O
23
20
18
17
15
16
O
13
14
12
24
O
2
22
21
3
5
7
8
9
11
4
6
10
OH
O

Fig. 2

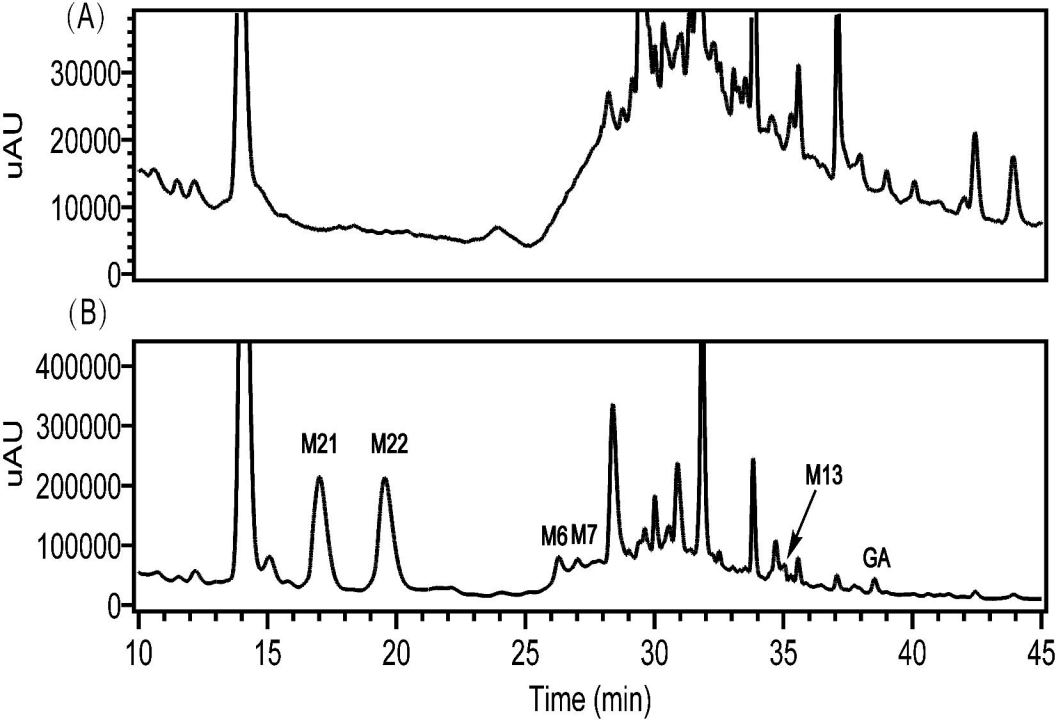
(A)
uAU
30000
20000
10000
0
(B)
uAU
400000
300000
200000
100000
0
M21
M22
M6
M7
M13
GA
10
15
20
25
30
35
40
45
Time (min)

Fig. 3

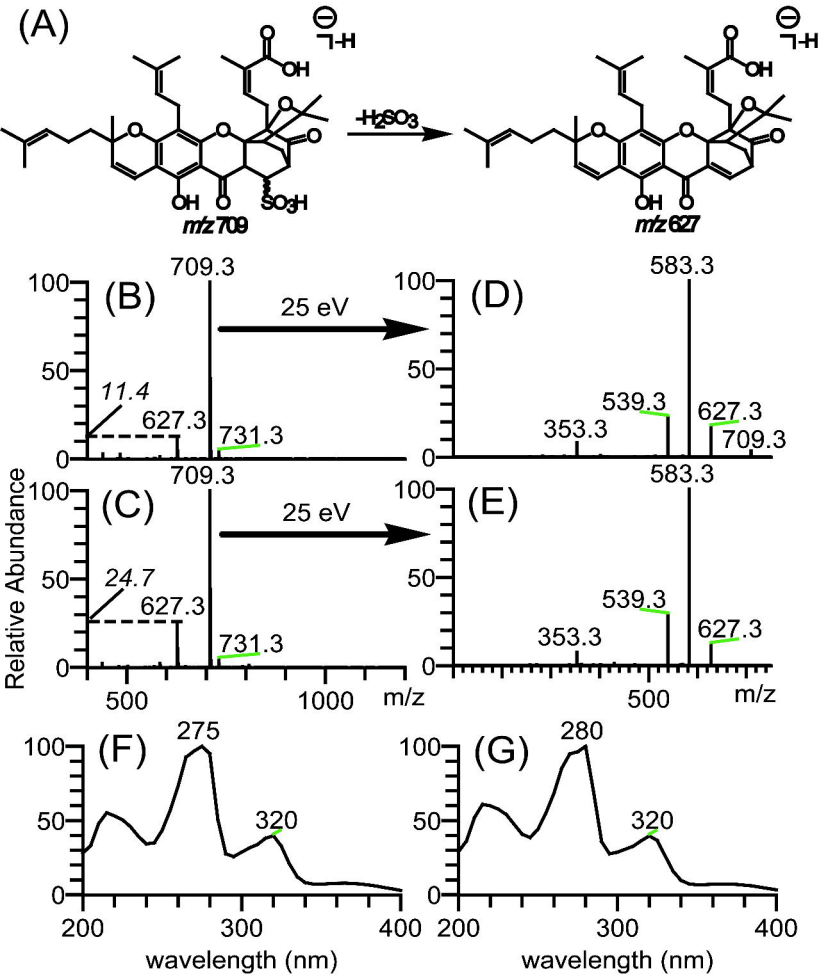
(A)
-H
OH
OH
O
O
SO3H
-H2SO3
m/z 709
m/z 627
(B)
709.3
25 eV
11.4
627.3
731.3
(D)
583.3
539.3
353.3
627.3
709.3
(C)
709.3
24.7
627.3
731.3
(E)
583.3
539.3
353.3
627.3
Relative Abundance
m/z
(F)
275
320
(G)
280
320
wavelength (nm)
wavelength (nm)

Fig. 4

(A)

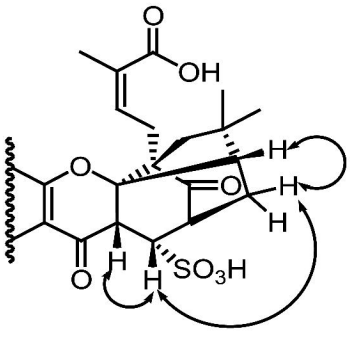

NOESY:

^1H ^1H

(B)

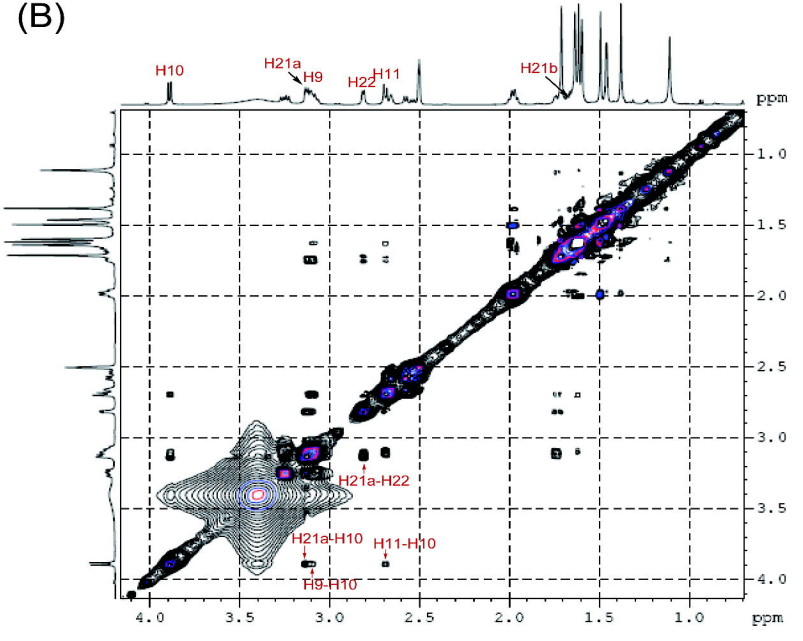

Fig. 5

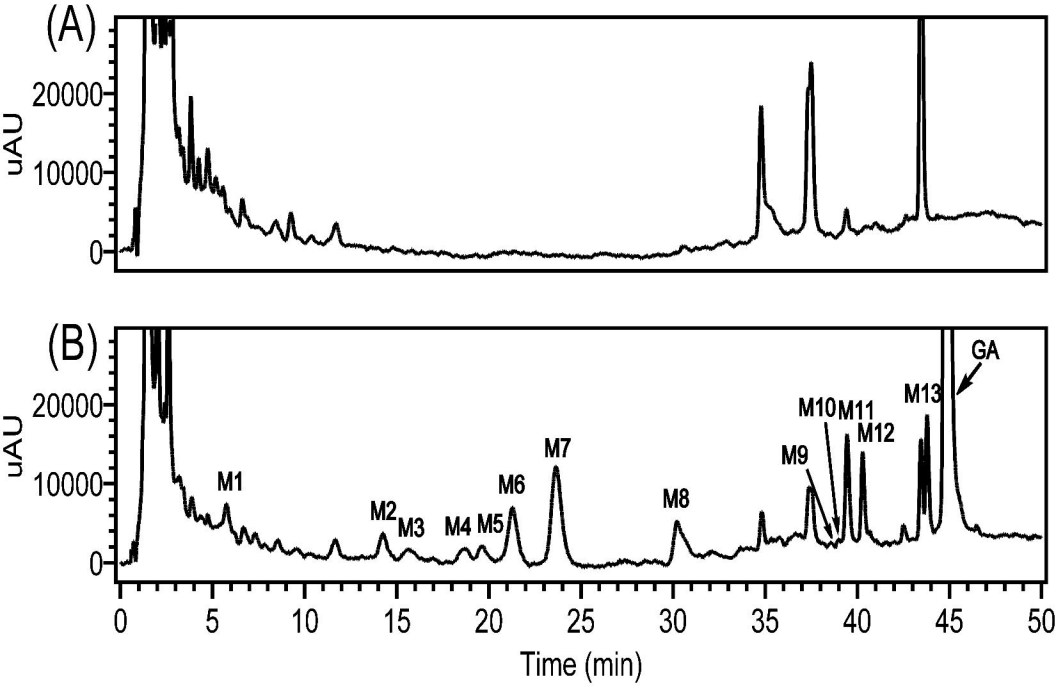
(A)
uAU
20000
10000
0
(B)
uAU
20000
10000
0
M1
M2
M3
M4
M5
M6
M7
M8
M9
M10
M11
M12
M13
GA
0
5
10
15
20
25
30
35
40
45
50
Time (min)

Fig. 6

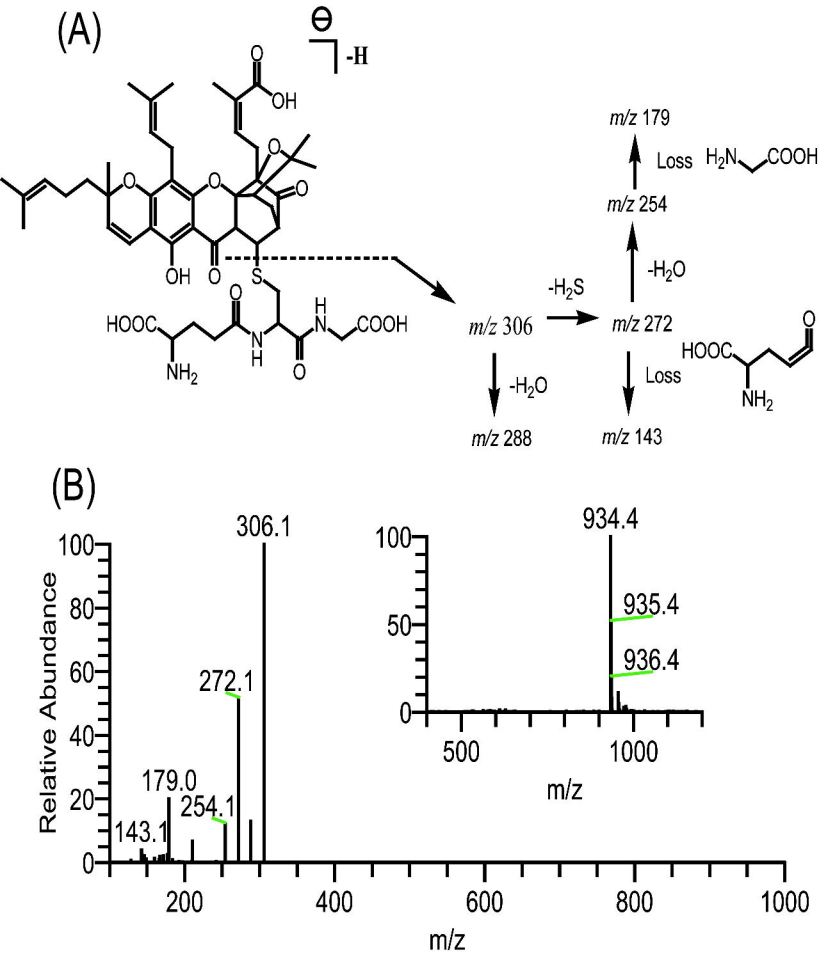
(A)
Θ
-H
OH
O
S
HOOC
NH2
N
H
COOH
-H2S
m/z 306
-H2O
m/z 288
m/z 272
-H2O
m/z 254
Loss
m/z 179
H2N
COOH
Loss
m/z 143
(B)
Relative Abundance
306.1
272.1
179.0
254.1
143.1
m/z
934.4
935.4
936.4
m/z

Fig. 7

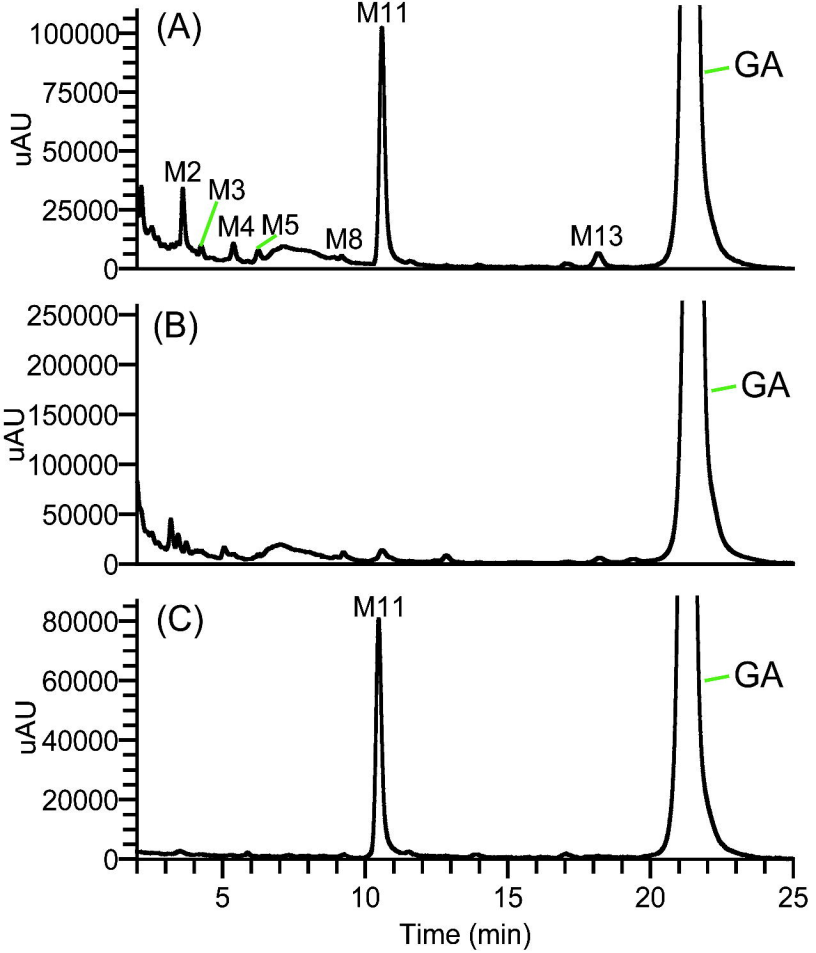
(A)
M11
GA
M2
M3
M4
M5
M8
M13
uAU
100000
75000
50000
25000
0
(B)
GA
uAU
250000
200000
150000
100000
50000
0
(C)
M11
GA
uAU
80000
60000
40000
20000
0
5
10
15
20
25
Time (min)

Fig. 8

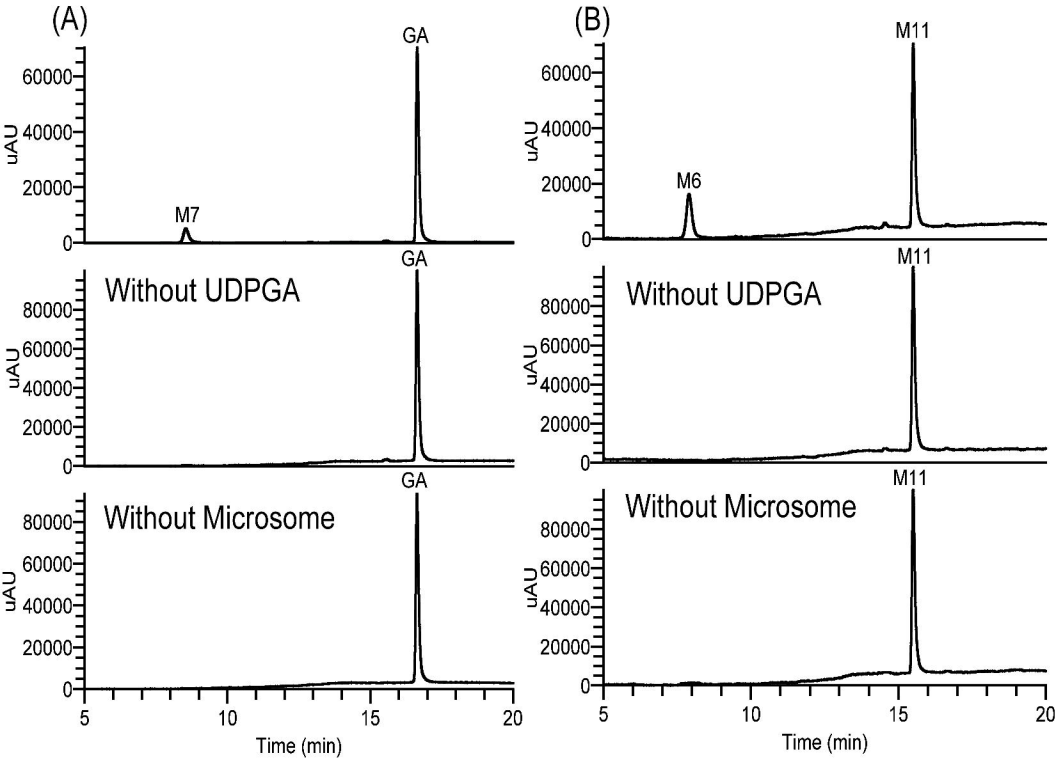
(A)
GA
M7
uAU
60000
40000
20000
0
Without UDPGA
GA
80000
60000
40000
20000
0
Without Microsome
GA
80000
60000
40000
20000
0
5
10
15
20
Time (min)
(B)
M11
M6
uAU
60000
40000
20000
0
Without UDPGA
M11
80000
60000
40000
20000
0
Without Microsome
M11
80000
60000
40000
20000
0
5
10
15
20
Time (min)

Fig. 9

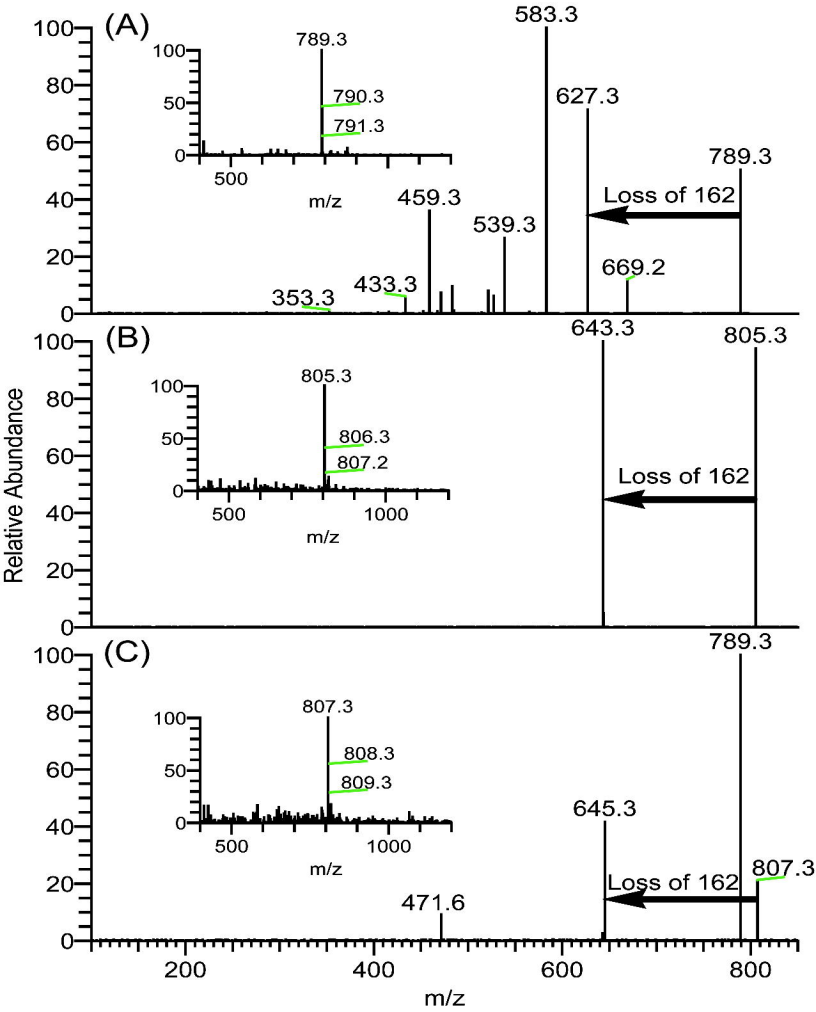
(A)
583.3
627.3
789.3
Loss of 162
459.3
539.3
669.2
433.3
353.3
789.3
790.3
791.3
m/z
(B)
643.3
805.3
Loss of 162
805.3
806.3
807.2
m/z
(C)
789.3
807.3
808.3
809.3
645.3
807.3
Loss of 162
471.6
m/z
Relative Abundance

Fig. 10

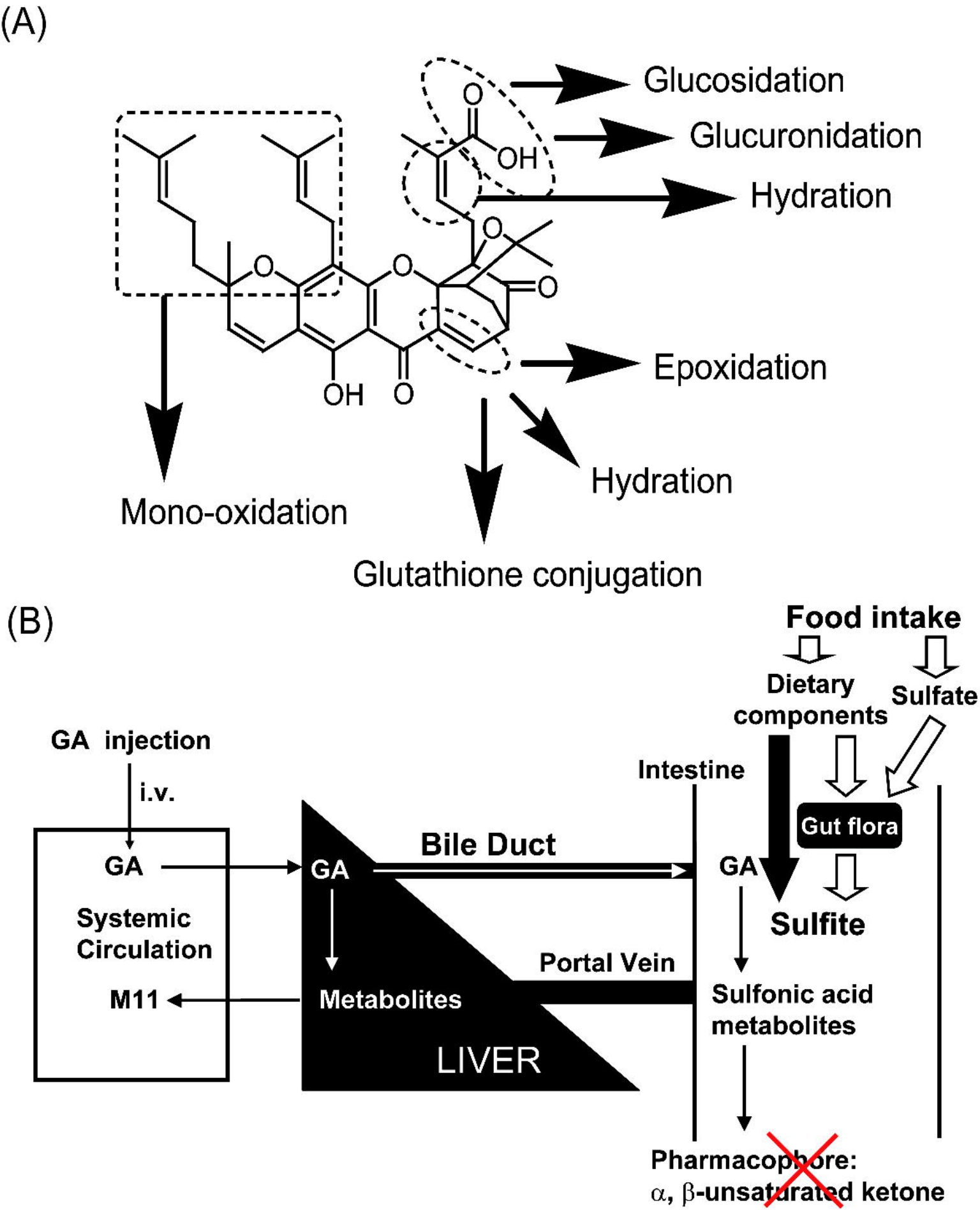
(A)
Glucosidation
Glucuronidation
Hydration
Epoxidation
Hydration
Mono-oxidation
Glutathione conjugation
(B)
Food intake
Dietary components
Sulfate
GA injection
i.v.
Intestine
Gut flora
Bile Duct
GA
GA
Sulfite
Systemic Circulation
Portal Vein
M11
Metabolites
Sulfonic acid metabolites
LIVER
Pharmacophore:
α, β-unsaturated ketone

Metabolism of Gambogic Acid in Rats: a Rare Intestinal Metabolic Pathway Responsible for its Final Disposition

Jing Yang, Li Ding, Linlin Hu, Wenjuan Qian, Shaohong Jin, Xiaoping Sun, Zhenzhong Wang, and Wei Xiao

Department of Pharmaceutical Analysis, Key Laboratory of Drug Quality Control and Pharmacovigilance, China Pharmaceutical University, Nanjing, China (*J.Y., L.D, L.H, W.Q.*), National Institution for the Control of Pharmaceutical and Biological Products, China (*S.J.*), and Kanion Pharmaceutical Co., Ltd, Lianyungang , China (*X.S, Z.W, W.X.*)

Supplemental experimental

***In vitro* rat intestinal contents incubation** The rats without dose were euthanized by cervical dislocation followed by removing the total intestinal tract immediately. The total intestinal contents of each rat were then collected and homogenized in 5 mL of water. The reactions were initiated by the addition of 100 μL of 1.0 mg/mL GA solution in the homogenate and carried out at 37 °C water bath. After approximately 24 h, 1.0 mL of sample from each tube was extracted with the same procedures as the plasma sample preparation, and then analyzed by LC-MS/MS. This experiment was performed in duplicate. The LC-MS/MS method was performed using an Agilent Technologies Series 6410B LC-MS/MS system (Agilent Technologies, Palo Alto, CA, USA), including an Agilent 1200 rapid LC system and an Agilent 6410B triple-quadrupole mass spectrometer equipped with an electrospray source. A Sepax HPC18 column, 3 μm, 150 × 2.1 mm i.d. (Sepax Technologies, Inc, Newark, USA) protected by a SecurityGuard C18 column, 5 μm, 4 × 2.0 mm i.d. (Phenomenex, Torrance, CA, USA) was used for all measurements. The Signal acquisition, peak integration and concentration determination were performed using the MassHunter supplied by Agilent Technologies. The mobile phase, delivered at a constant flow rate of 0.25 mL/min, consisted of a gradient of solvent A (acetonitrile) in solvent B (10 mM ammonium acetate in water), as follows: 0 to 15 min, 50 % A; 20 to 45 min, 90 % A; 45.1 to 60 min, 50 % A. The column temperature was maintained at 25 °C. The triple-quadrupole mass spectrometer equipped with an ESI source was set with the drying gas (N_2) flow of 10 L/min, nebulizer pressure of 40 psig, drying gas

temperature of 350 °C, capillary voltage of 3.5 kV and the negative ion mode. The fragmentor voltage was set at 140 V. The ESI-MS was performed in the selected-ion monitoring (SIM) mode using the target ions of m/z 709.3 for M21 and M22, full scan mode, and product ion scanning mode, respectively.

Study of the *in vitro* formation mechanism of M11 Incubations with NADPH consisted of GA (50 μM), and NADPH (0.1, 1, and 10 mM) in 0.2 mL of 0.1 M PBS buffer (pH 7.4). GA in 5.0 μL of acetonitrile was added to the incubation tubes containing NADPH solution. After mixing, the tubes were incubated for 1 h at 37 °C with air and without oxygen (Expelling the air with a gentle N_2 stream), respectively. All incubations were performed in triplicate. The incubation was stopped by adding 1mL ethyl acetate. Following centrifugation and separation, the organic phase was evaporated to dryness under a stream of nitrogen in a water bath of 40 °C. The residue was reconstituted in 150 μL of mobile phase, and a 20 μL aliquot was injected into the HPLC system. The HPLC analysis was performed using an Agilent 1100 system (Agilent Technologies, Palo Alto, CA, USA). A Venusil C18 column, 5 μm, 250 × 4.6 mm i.d. (Agela Technologies, Newark, DE, USA) protected by a SecurityGuard C18 column, 5 μm, 4 × 3.0 mm i.d. (Phenomenex, Torrance, CA, USA) was used for all measurements. The Signal acquisition, peak integration and concentration determination were performed using the ChemStation software (10.02 A) supplied by Agilent Technologies. The mobile phase was 10 mM ammonium acetate water solution - acetonitrile (10:90, v/v) at a flow rate of 1.5 mL/min. The column

temperature was maintained at 25°C. M11 was measured at 320 nm.

Legends of supplemental Figures:

Fig.S1 Full scan MS^2 chromatograms of the synthesized reference standards of M21(A) and M22 (B), and the fecal sample after 4 mg/kg i.v. dose.

Fig.S2 Typical SIM chromatogram of M21 and M22 in the rat intestinal contents incubation sample.

Fig.S3 Proposed fragmentation pathway of M1 (A) and the product ion scanning spectrum (B) in the positive ion ESI mode (Inset) the Q1 full scan spectrum of M1.

Fig.S4 Expanded region of the chemical shifts exhibiting the glutathionyl group in the ^{1}H-NMR spectrum (A) and ^{13}C-NMR of 10-GGA (M1 reference) in DMSO-d_6.

Fig.S5 Proposed fragmentation pathway of the mono-oxidation products of GA (A) and M4 (B) in the negative ion ESI mode

Fig.S6 Typical chromatograms of blank plasma (A) and a plasma sample during 0-4 h after an 4mg/kg i.v. dose (B)

Fig.S7 The effect of condition with O_2 and without O_2 on the formation of M11. Data expressed as mean ± S.D., n=3. * $p < 0.01$.

Fig.S8 Proposed fragmentation pathway of M7 (A) and the product ion scanning spectra of M7 (B) and M6 (C) in the negative ion ESI mode. Inset: the Q1 full scan spectra of M7 and M6.

Fig.S9 Typical chromatograms for glucuronides of GA (A) and M11 (B) treated at different conditions after *in vitro* incubation, respectively.

Fig.S1

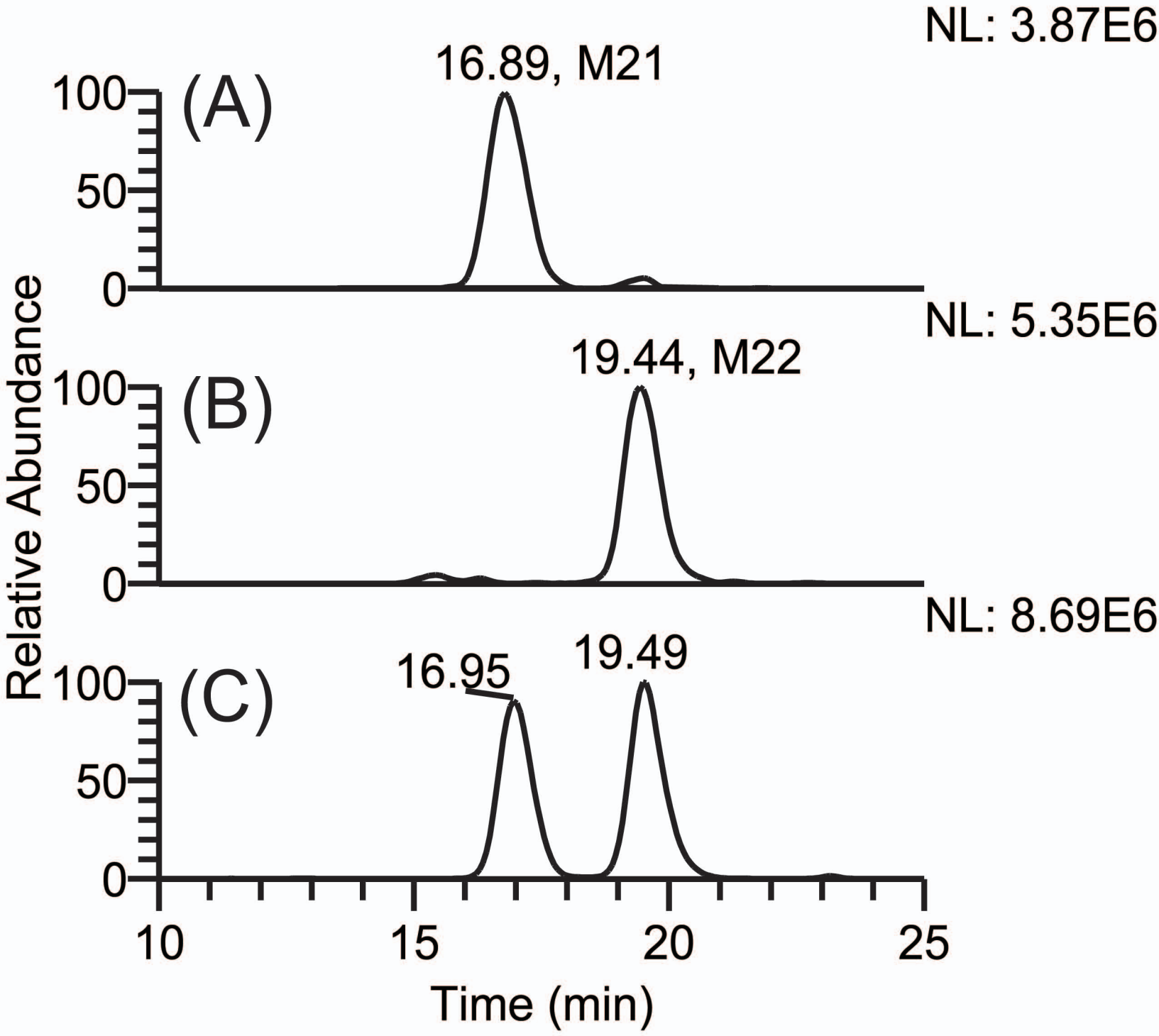
NL: 3.87E6
16.89, M21
100
(A)
50
0
NL: 5.35E6
19.44, M22
100
(B)
50
0
NL: 8.69E6
16.95
19.49
100
(C)
50
0
Relative Abundance
10
15
20
25
Time (min)

Fig.S2

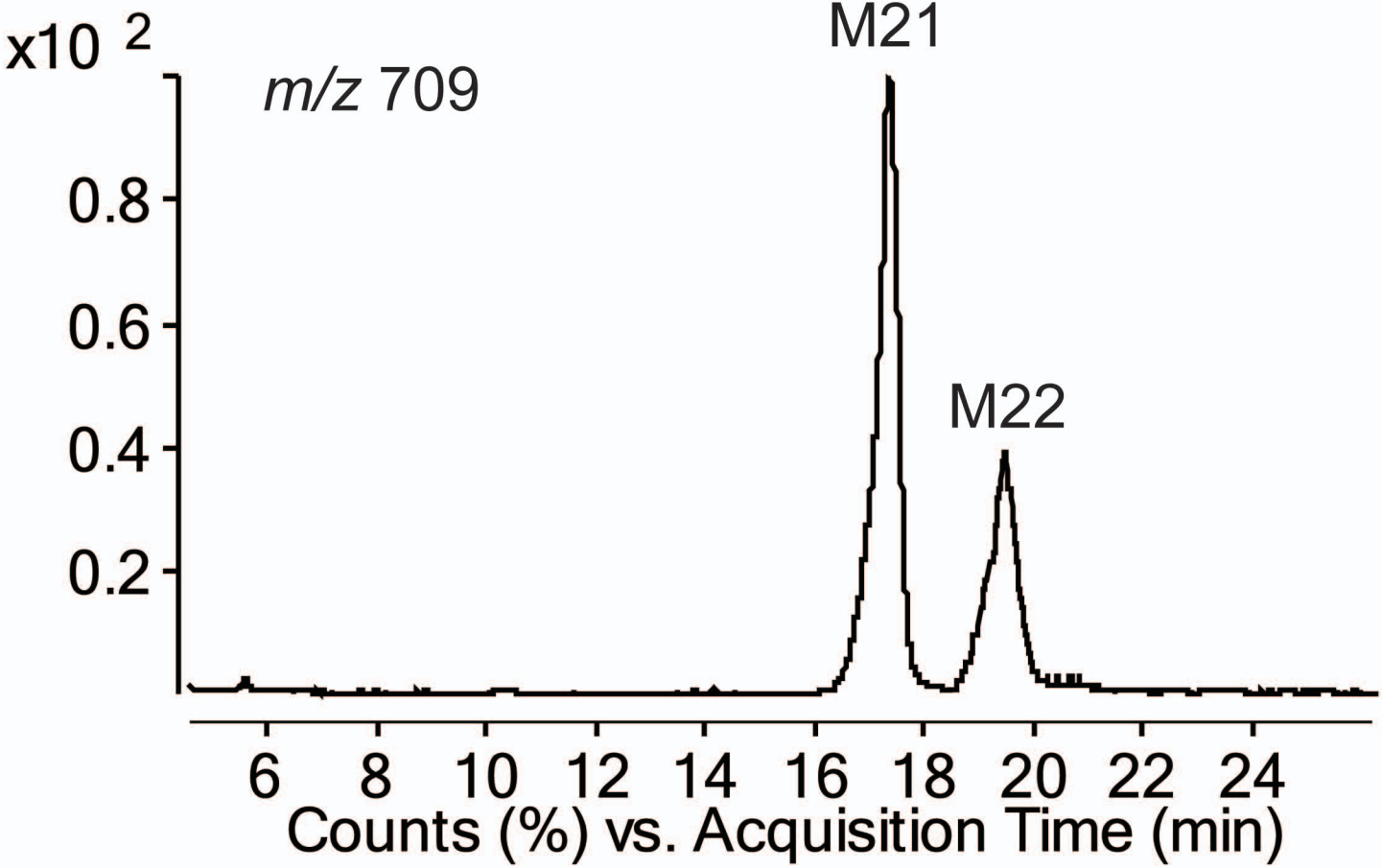
x10 2
m/z 709
M21
M22
0.8
0.6
0.4
0.2
6
8
10
12
14
16
18
20
22
24
Counts (%) vs. Acquisition Time (min)

Fig S3

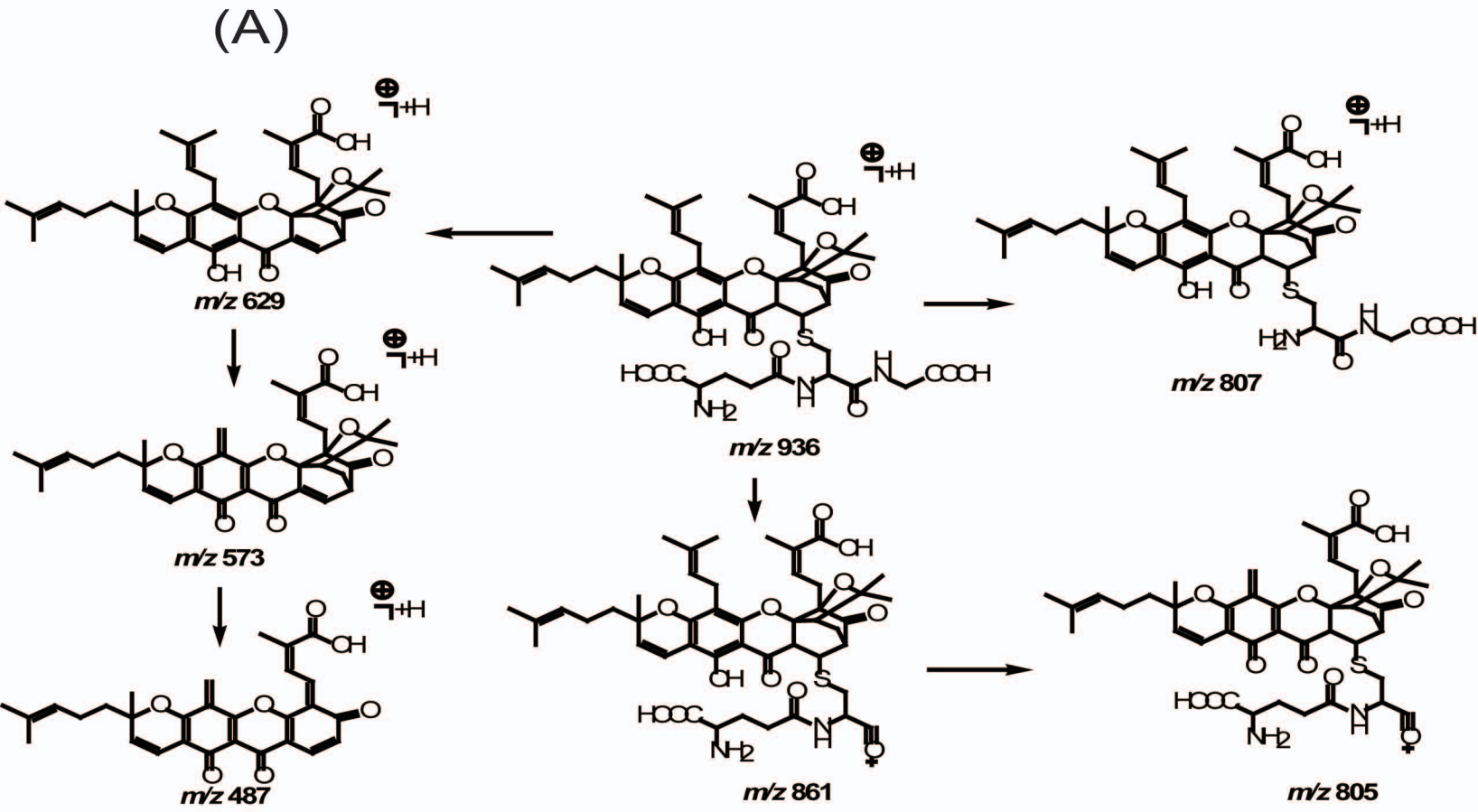
(A)
m/z 629
m/z 936
m/z 807
m/z 573
m/z 487
m/z 861
m/z 805

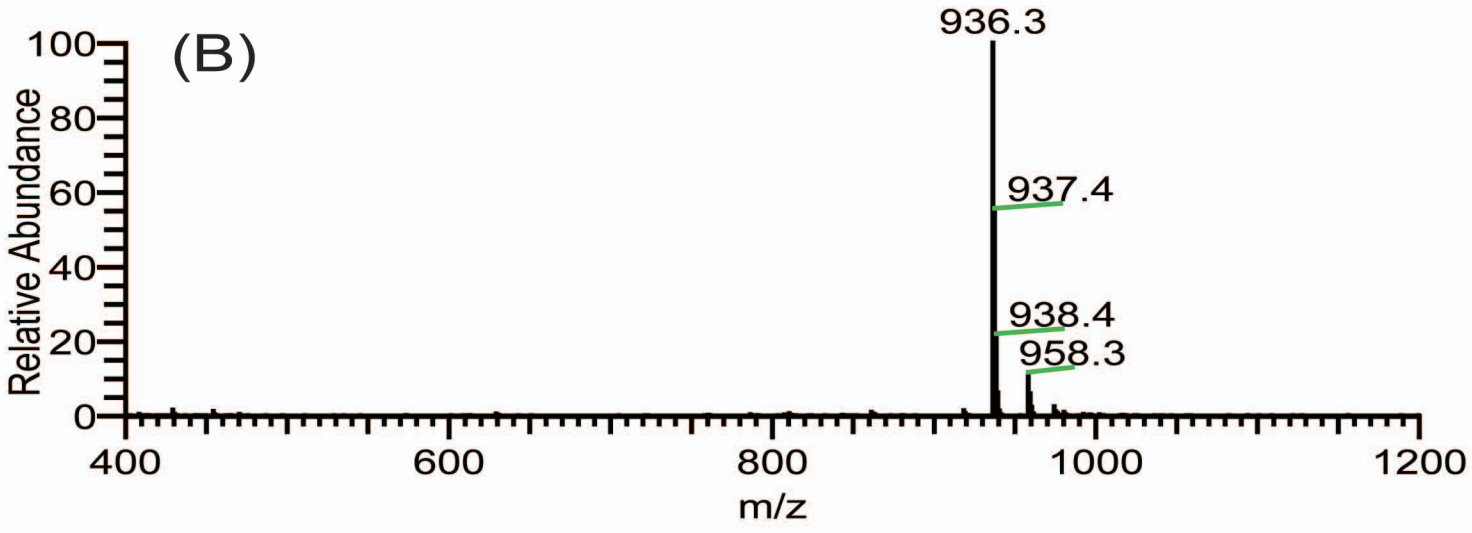
(B)
936.3
937.4
938.4
958.3
Relative Abundance
m/z

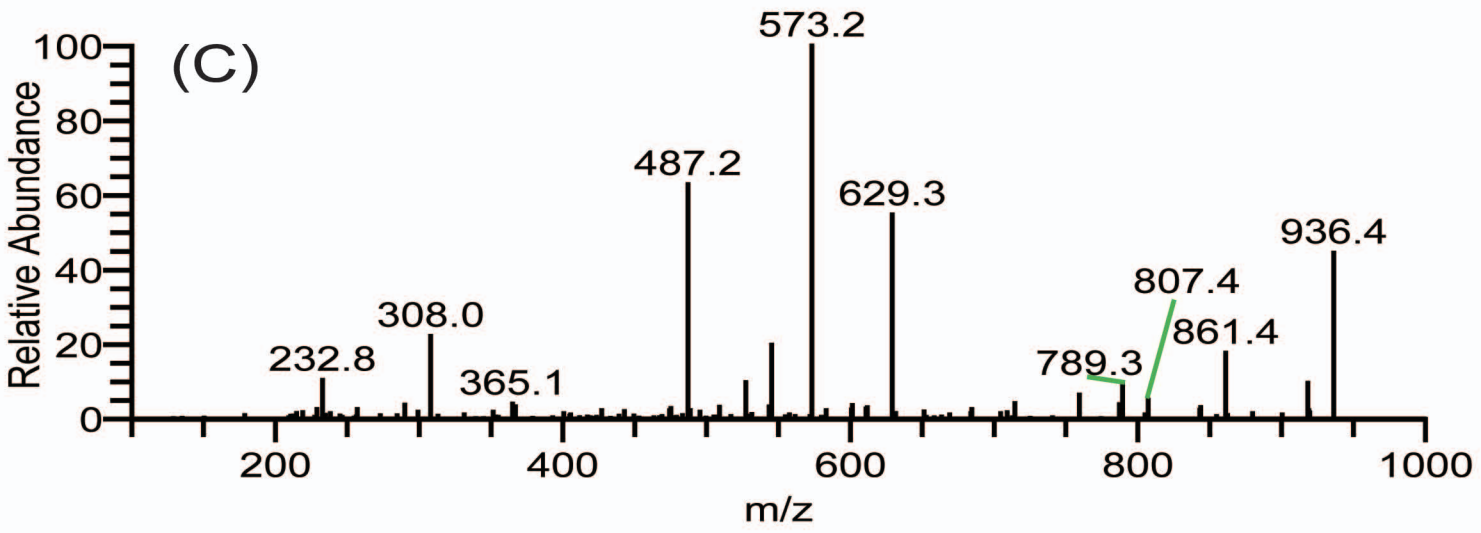
(C)
573.2
487.2
629.3
936.4
807.4
861.4
308.0
232.8
365.1
789.3
Relative Abundance
m/z

Fig.S4

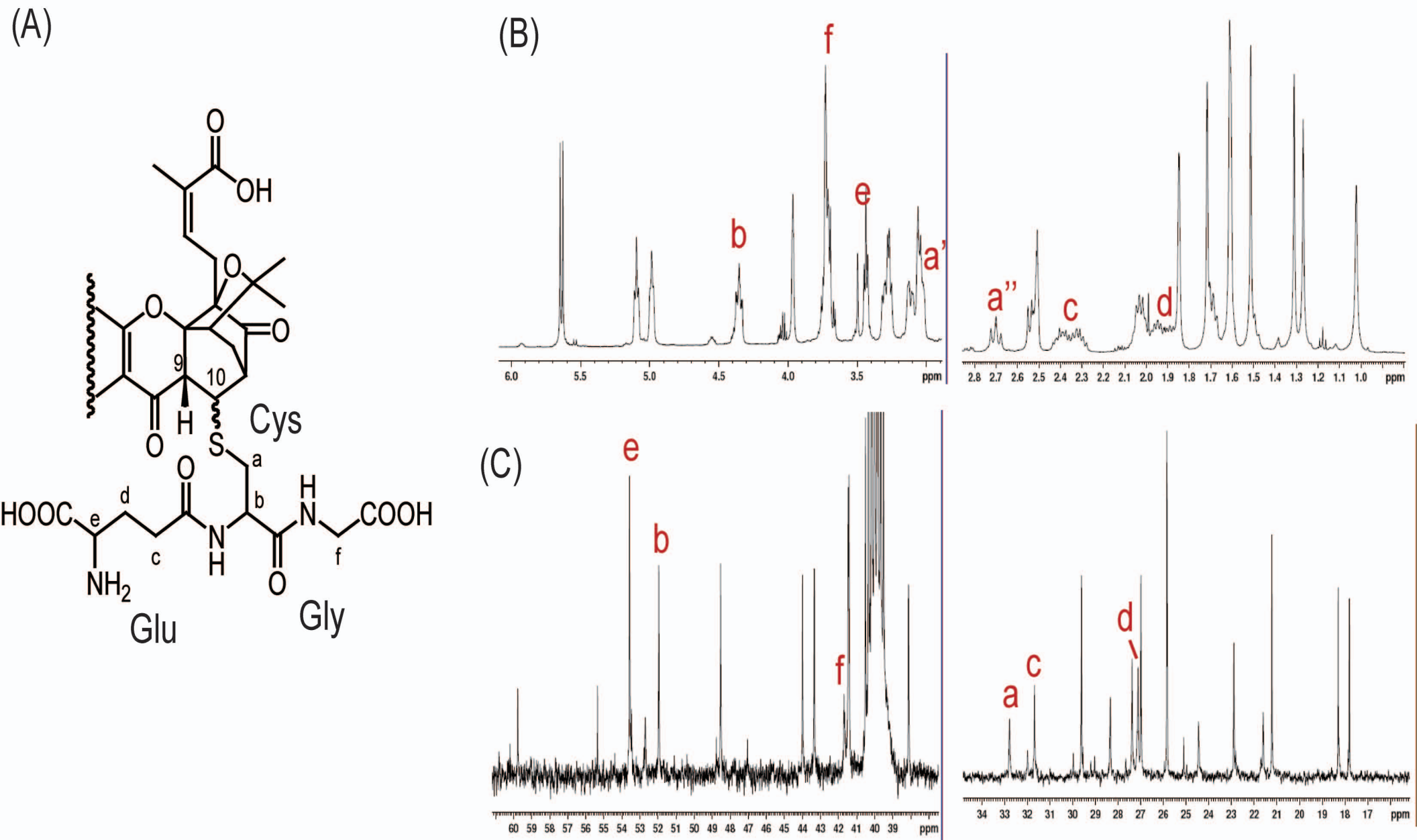
(A)
O
OH
O
O
O
9
10
H
O
Cys
S
a
HOOC
e
d
b
H
N
COOH
O
N
H
c
f
NH2
O
Glu
Gly
(B)
f
b
e
a'
a''
c
d
6.0 5.5 5.0 4.5 4.0 3.5 ppm
2.8 2.7 2.6 2.5 2.4 2.3 2.2 2.1 2.0 1.9 1.8 1.7 1.6 1.5 1.4 1.3 1.2 1.1 1.0 ppm
(C)
e
b
f
a
c
d
60 59 58 57 56 55 54 53 52 51 50 49 48 47 46 45 44 43 42 41 40 39 ppm
34 33 32 31 30 29 28 27 26 25 24 23 22 21 20 19 18 17 ppm

Fig.S5

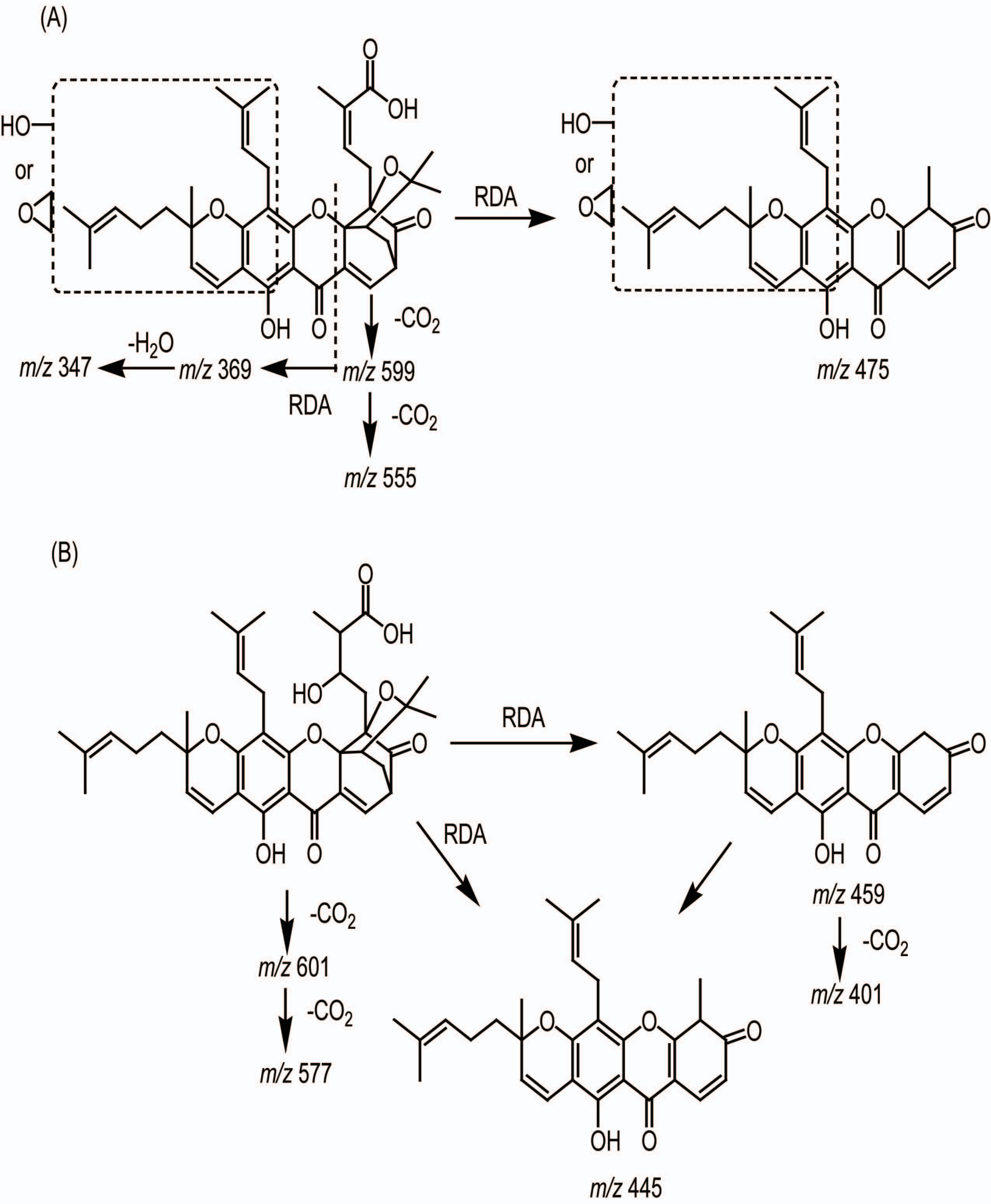
(A)
HO
or
O
OH
O
O
O
O
O
O
OH
O
RDA
HO
or
O
O
O
O
O
OH
O
-CO2
-H2O
m/z 347
m/z 369
m/z 599
RDA
-CO2
m/z 555
m/z 475
(B)
O
OH
HO
O
O
O
O
OH
O
RDA
RDA
-CO2
m/z 601
-CO2
m/z 577
m/z 459
-CO2
m/z 401
OH
O
m/z 445

Fig.S6

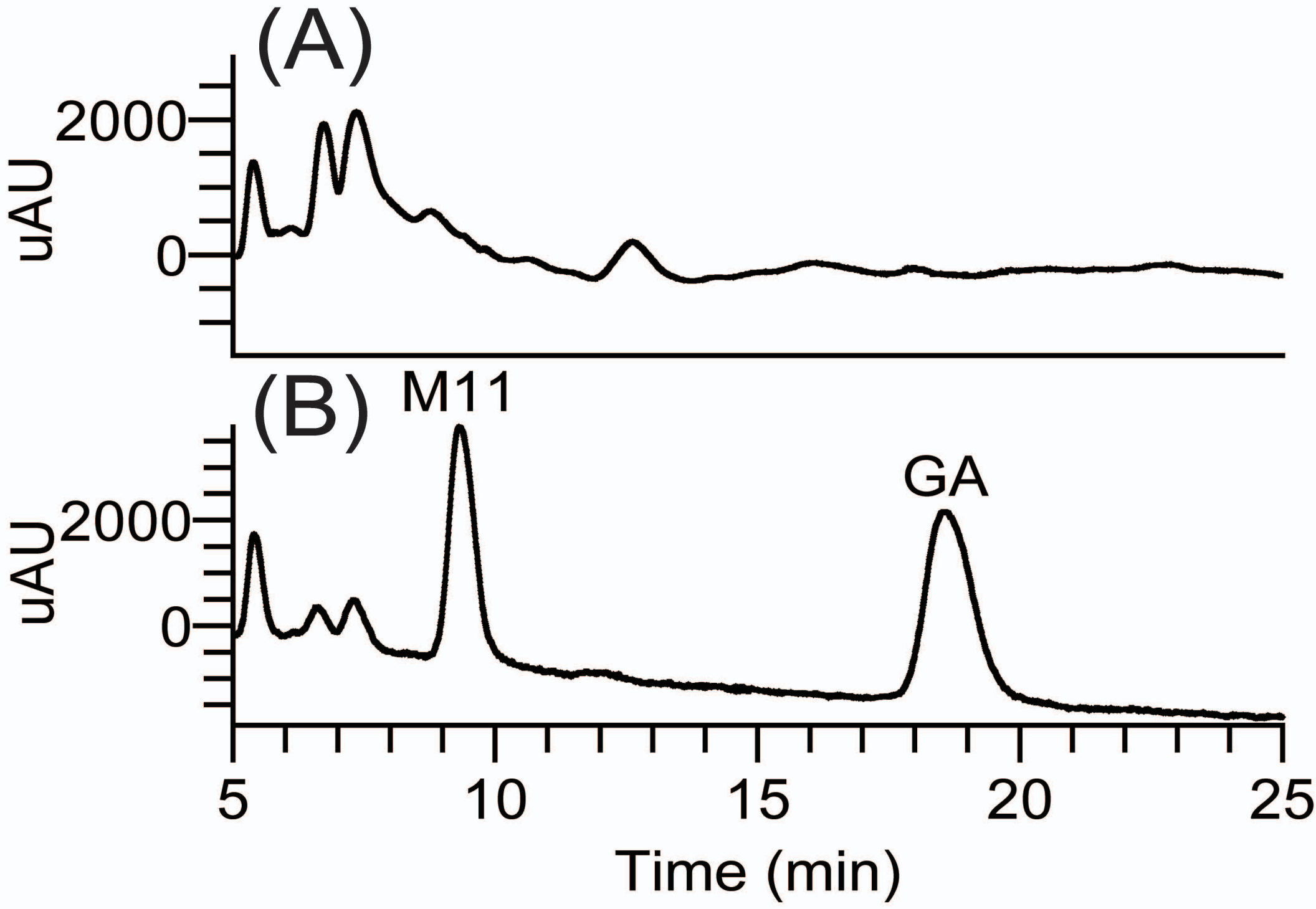

Fig.S7

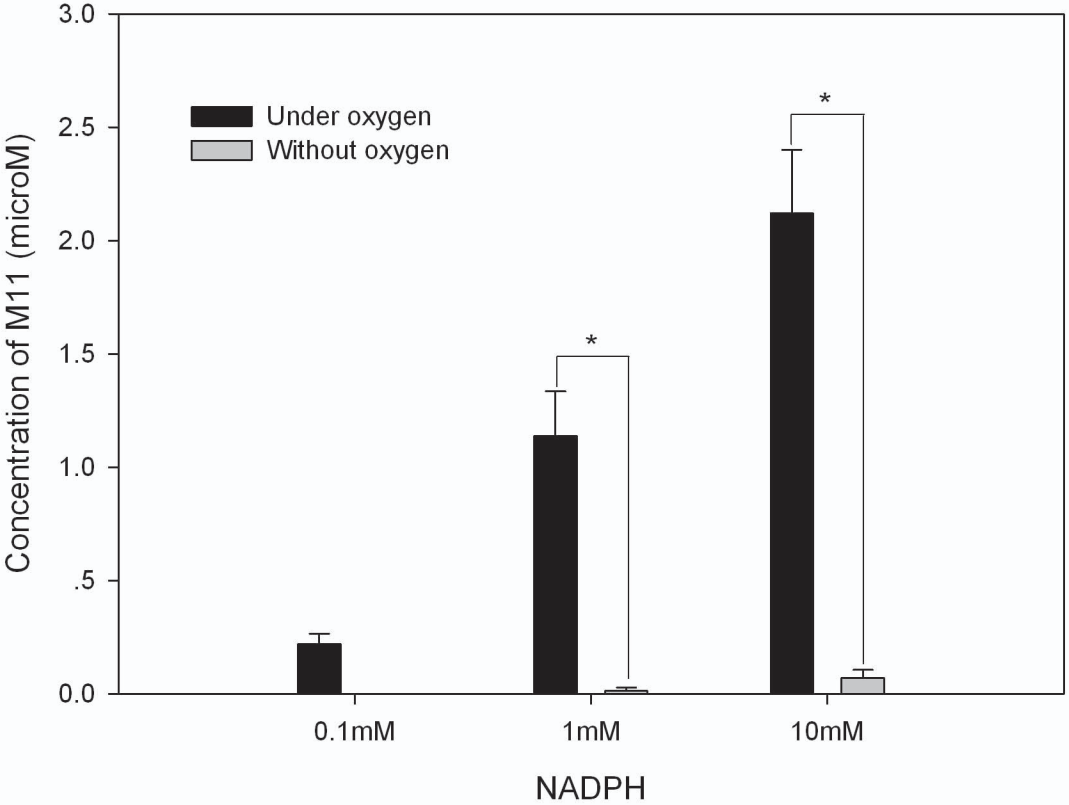
3.0
2.5
2.0
1.5
1.0
.5
0.0
Concentration of M11 (microM)
Under oxygen
Without oxygen
*
*
0.1mM
1mM
10mM
NADPH

Fig.S8

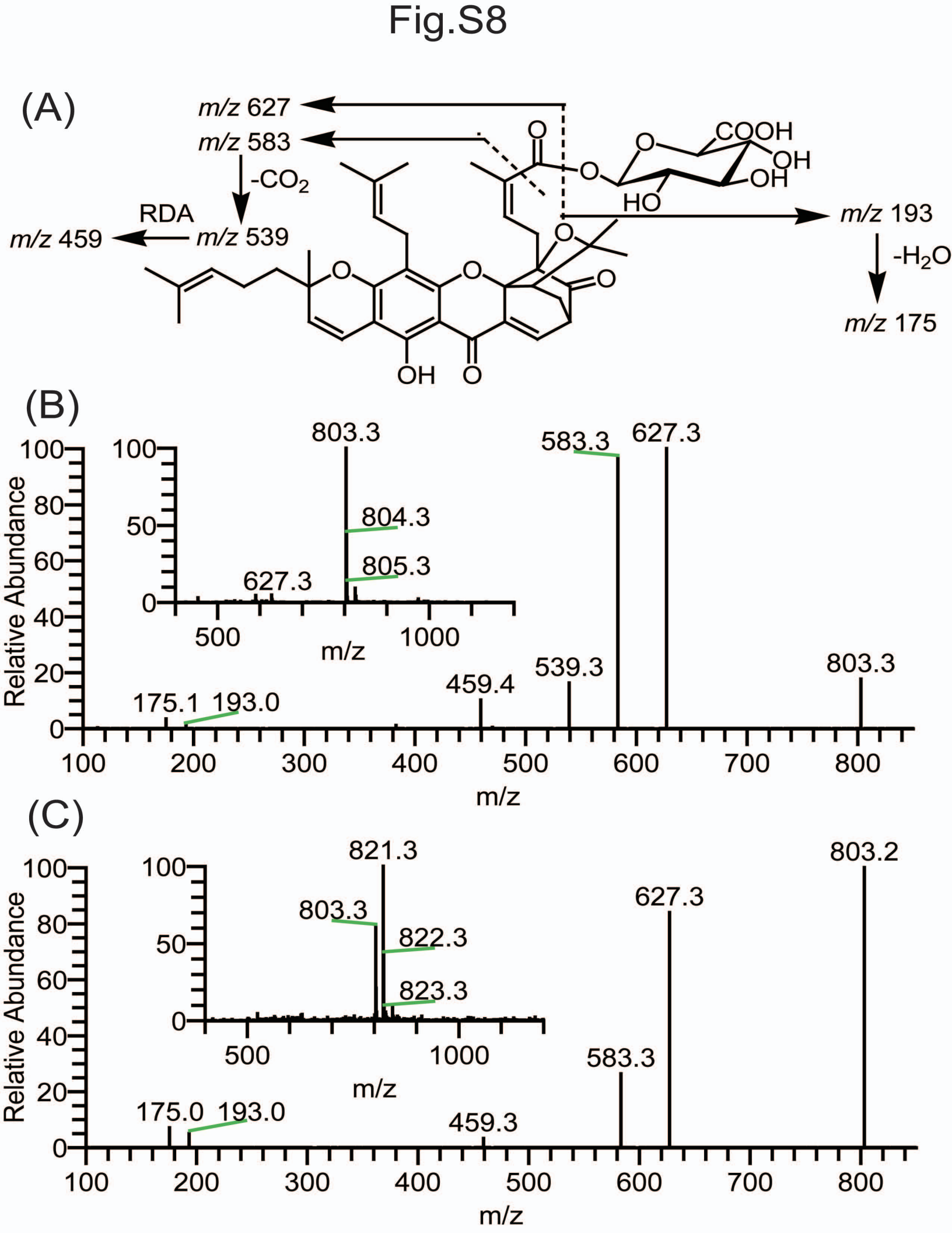
(A)
m/z 627
m/z 583
-CO2
RDA
m/z 459
m/z 539
m/z 193
-H2O
m/z 175
COOH
OH
OH
HO
O
OH
(B)
803.3
583.3
627.3
804.3
805.3
627.3
539.3
459.4
175.1
193.0
803.3
Relative Abundance
m/z
(C)
821.3
803.2
627.3
803.3
822.3
823.3
583.3
175.0
193.0
459.3
Relative Abundance
m/z

Fig.S9

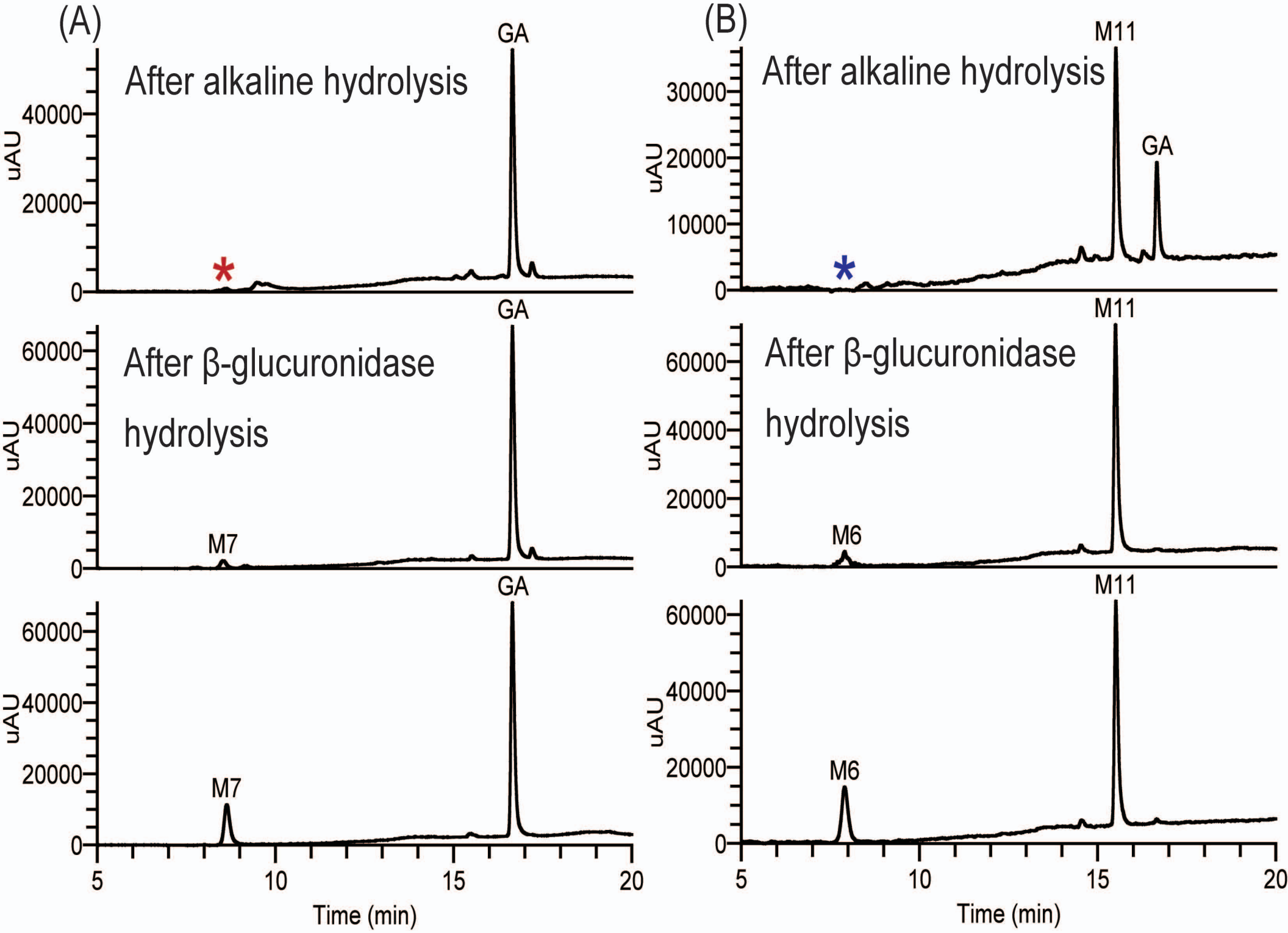
(A)
After alkaline hydrolysis
GA
*
After β-glucuronidase hydrolysis
GA
M7
GA
M7
uAU
40000
20000
0
60000
Time (min)
5
10
15
20
(B)
After alkaline hydrolysis
M11
GA
*
30000
10000
After β-glucuronidase hydrolysis
M11
M6
M11
M6